

# Mechanical, Hygroscopic, and Thermal Properties of Ultrathin Polymeric Substrates for Magnetic Tapes

Tiejun Ma, Bharat Bhushan

*Nanotribology Laboratory for Information Storage and MEMS/NEMS, The Ohio State University, 206 West 18th Avenue, Columbus, Ohio 43210*

Received 30 September 2002; accepted 22 December 2002

**ABSTRACT:** Mechanical, hygroscopic, and thermal properties of improved ultrathin polymeric films for magnetic tapes are presented. These films include poly(ethylene terephthalate) (PET), poly(ethylene naphthalate) (PEN), and aromatic polyamide (ARAMID). PET films are currently the most commonly used polymeric substrate material for magnetic tapes, followed by PEN and ARAMID. The thickness of the films ranges from 6.2 to 4.8  $\mu\text{m}$ . Tensile tests were run to obtain the Young's modulus, F5 value, strain at yield, breaking strength, and strain at break. The storage modulus,  $E'$ , and the loss tangent,  $\tan \delta$ , were measured using a dynamic mechanical analyzer (DMA) at temperature ranges of  $-50$  to  $150^\circ\text{C}$  (for PET) and  $-50$  to  $210^\circ\text{C}$  (for PEN and ARAMID) and at a frequency range of 0.016–28 Hz. Frequency–temperature superposition was used to predict the dynamic mechanical behavior of the films over a 28-decade frequency range. Short-term longitudinal creep behavior of the films

during 10, 30, 60, and 300 s, 7 MPa, were measured at 25 and  $55^\circ\text{C}$ . Long-term longitudinal creep measurements were performed at 25, 40, and  $55^\circ\text{C}$  for 100 h. The Poisson's ratio and 50-h long-term lateral creep were measured at  $25^\circ\text{C}/15\%$  RH,  $25^\circ\text{C}/50\%$  RH,  $25^\circ\text{C}/80\%$  RH, and  $40^\circ\text{C}/50\%$  RH. The in-plane coefficient of hygroscopic expansion (CHE) at  $25^\circ\text{C}/20$ – $80\%$  RH and the coefficient of thermal expansion (CTE) at  $30$ – $70^\circ\text{C}$  were measured for all the samples. The properties for all films are summarized. The relationship between the polymeric structure and the mechanical and physical properties are discussed, based on the molecular structure, crystallinity, and molecular orientation. © 2003 Wiley Periodicals, Inc. *J Appl Polym Sci* 89: 3052–3080, 2003

**Key words:** plastics; thin films; mechanical properties; thermal properties

## INTRODUCTION

Magnetic tapes provide extremely high volumetric density, high data rates, and low cost per megabyte compared to other storage media.<sup>1</sup> For example, the Generation 4 Ultrium format LTO (Linear Tape Open) tape provides for up to 1.6 TB in a single cartridge, with a compressed data rate to 320 MB per second.<sup>2</sup> The tape drives are primarily used for data backup and for some high-volume recording devices, such as instrument and satellite recorders.

Thinner substrates and higher areal densities (track density  $\times$  linear density) are required to meet the demand for advanced magnetic storage devices with high volumetric densities, especially for computer data storage tapes. For higher areal densities, a substrate with high dimensional stability under various environmental conditions is required. Longitudinal recording is sensitive to changes in the distance of the tracks from the tape edge while

helical scan recording is sensitive to the track angle relative to the tape edge. The track parameters are changed due to dimensional changes in the machine direction (MD) and transverse direction (TD). If the storage device is a linear tape drive, specifically for high track densities, lateral deformation of the substrates due to viscoelastic, thermal, hygroscopic, and shrinkage effects must be minimal during storage on a reel and use in a drive. In a linear tape drive, any linear deformations can be accounted for by a change in the clocking speed. However, if the storage device is a rotary tape drive, anisotropic deformation would be undesirable. Therefore, substrates for the linear tape drives are tensilized more in the MD than in the TD to provide high modules in the MD and low contraction in the TD, whereas substrates for rotary tape drives are tensilized about the same both in the MD and the TD or slightly tensilized along the TD. To minimize stretching and damage during manufacturing and use, the thinner substrates should be a high-modulus and high-strength material with low-creep characteristics. Furthermore, since high coercivity magnetic films on metal-evaporated tapes are deposited and/or heat-treated at elevated temperatures, a substrate with stable mechanical properties to  $100$ – $150^\circ\text{C}$  or even higher is desirable.

Correspondence to: B. Bhushan (bhushan.2@osu.edu).

Contract grant sponsor: Nanotribology Laboratory for Information Storage and MEMS/NEMS (NLIM), Ohio State University.

Viscoelasticity refers to the combined elastic and viscous deformation of a substrate when external forces are applied, and shrinkage occurs when residual stresses present in the substrate are relieved at elevated temperatures. If a substrate of a magnetic tape shrinks or deforms viscoelastically, then the head cannot read information stored on the tape. Various long-term reliability problems including uneven tape-stack profiles (or hardbands), mechanical print-throughs, instantaneous speed variations, and tape stagger problems can all be related to the viscoelastic property of substrates.<sup>1</sup> To minimize these reliability problems, it is not only important to minimize creep strain, but the rate of increase of total strain also needs to be kept to a minimum to minimize relaxation of wound-in tension in a reel. The elastic and viscoelastic behavior of the substrate is also important to determine how the tape responds as it is unwound from the reel and travels over the head. This elastic/viscoelastic recovery and subsequent conformity of the tape with the head occurs in just a few milliseconds and requires optimization of the substrate's dynamic properties. Elastic, viscoelastic, and shrinkage measurements have been performed on various substrates by various investigators.

Reversible damage (due to elastic, thermal, and hygroscopic effects) during storage can be overcome by exercising the reel. Furthermore, it is desirable to match thermal expansion of the substrate with that of the head substrate, commonly used  $\text{Al}_2\text{O}_3\text{—TiC}$ , which is about  $7 \times 10^{-6}/^\circ\text{C}$ . Hygroscopic expansion should be as close to zero as possible. As far as the finished tape is concerned, physical properties of both substrate and magnetic/nonmagnetic layers affect the properties of a tape and should be taken into account. Since the polymeric substrate takes up 75–90% of the total thickness, its dimensional stability is the key. Both substrate and coating thicknesses are expected to decrease with time; however, the coating-to-substrate thickness ratio is not expected to change much.

As an example, for a linear magnetic tape storage device with a volumetric density of 1 terabyte per cubic inch, the following characteristics may be required: a substrate which is approximately  $4 \mu\text{m}$  thick, a magnetic medium with a track density of about 360 tracks/mm with a 64 head array and eight head positions, and a linear density of about 64 kbits/mm. Because of limitations in the fabrication of narrow track heads, data can be read from only 256 tracks while scanning in a data recovery mode. Therefore, for a 12.7-mm-wide tape, if a 10% track mismatch is tolerable, lateral deformation (both reversible and irreversible) of less than about  $5 \mu\text{m}$  in the TD is desirable, provided that the head can be recentered.<sup>1</sup> So, the ultimate drive error performance is impacted by lateral tape motion and track spacing variation due to dimensional changes in the tape.<sup>3</sup> Controlling the track spacing requires better understanding of the dimensional stability of the polymeric substrate and

**TABLE I**  
**List of Magnetic Tape Substrates Used in This Study**

Sample	Symbol	Thickness ( $\mu\text{m}$ )
Standard PET	Standard PET	14.0
Tensitized PET	T-PET(1)	6.1
Tensitized PET	T-PET(2)	6.1
Supertensitized PET	ST-PET	6.1
Standard PEN	Standard PEN	6.2
Tensitized PEN	T-PEN	6.2
Supertensitized PEN	ST-PEN	6.2
ARAMID	ARAMID	4.8

how it is influenced by pack stresses, environmental changes (such as temperature and humidity changes), and tape design and processing. The current dimensional stability budget for reversible and irreversible changes (due to elastic, thermal, hygroscopic, viscoelastic, and shrinkage effects) in year 2002 is about 1200 ppm and is expected to be lower than 400 ppm for the terabyte per cubic inch capacity tape.

Poly(ethylene terephthalate) (PET) is currently the most widely used polymeric substrate material for magnetic tapes, followed by poly(ethylene naphthalate) (PEN) and aromatic polyamide (ARAMID). The second author's group has extensively studied the viscoelastic properties and dimensional stability of the above ultrathin polymeric films<sup>1,4–8</sup> as well as magnetic and nonmagnetic layers.<sup>9–12</sup> This includes the tensile and dynamic mechanical and thermal expansion behavior using commercial testers, longitudinal creep and shrinkage using a creep apparatus, Poisson's ratio, and thermal and hygroscopic expansion for some films using a laser scanning microscope (LSM) apparatus.

The objective of this study was to provide a perspective of the mechanical, hygroscopic, and thermal properties for various polymeric films of interest for the magnetic tape substrates. Data from various tests on eight polymeric films include tensile tests, DMA tests, short-term and long-term longitudinal creep tests, Poisson's ratio, and long-term lateral creep tests, coefficient of hygroscopic expansion (CHE) tests, and coefficient of thermal expansion (CTE) tests. The storage modulus and lateral creep for four tape substrates and corresponding virgin films were measured to evaluate the degradation of the substrate after tape manufacturing. The physical and mechanical properties of the polymeric films are summarized; the relationship among the molecular structure, tensilization processing, and the properties of the polymeric films are discussed.

## EXPERIMENTAL

### Experimental samples

Table I provides a list of the polymeric films examined in this study along with their thicknesses. PET films

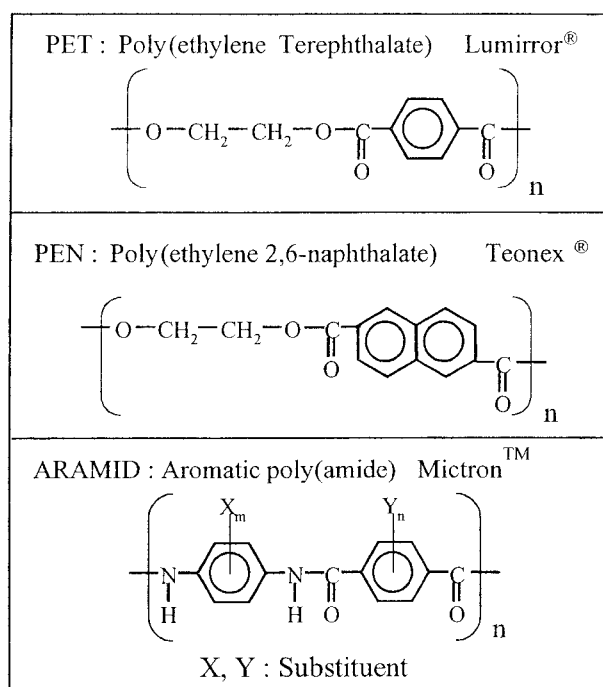


Figure 1 Chemical unit structures of polymeric films.

include four kinds of films: standard PET, tensilized PET(1) and (2), and supertensilized PET. A 14- $\mu\text{m}$ -thick standard PET film is the typical substrate used for videotapes. Various 6.1- $\mu\text{m}$ -thick tensilized-type PET films, which include tensilized PET(1) and (2) and supertensilized PET, drawn to different degrees of tensilization in the MD, are commonly used for computer data storage tapes. PEN films have 6.2- $\mu\text{m}$  thickness and include three kinds of films: standard PEN, tensilized PEN, and supertensilized PEN, with different degrees of tensilization in the MD. PEN films are also used for long-play videotapes and computer data storage tapes. ARAMID film has a 4.8- $\mu\text{m}$  thickness used for magnetic tapes with thinner substrates. The samples are available as commercial films except supertensilized PET. Both PET and PEN films are manufactured by a biaxial drawing process. Standard PET is drawn biaxially by the ratio of approximately four times in both the MD and the TD during processing.<sup>6</sup> For PET and PEN, more tensilization leads to higher values of the modulus and strength and less shrinkage. On the other hand, ARAMID film is manufactured using a solution-casting process and then drawn slightly using a drawing process, which makes it more expensive than is PET film ( $\sim 3\times$ ); PEN film is also slightly more expensive than PET film ( $\sim 1.3\times$ ). The symbols in Table I are used throughout the article.

The polymeric unit structure of the three types of substrates is illustrated in Figure 1. PET and PEN have identical hydrocarbon backbones indicative of polyester materials. PET contains a single benzene ring in each repeating unit, whereas PEN contains a naphtha-

lene ring that is slightly more rigid. PET and PEN films are semicrystalline materials with the typical crystallinities of 40–50% and 30–40%, respectively.<sup>6</sup> ARAMID has rigid rodlike structures that exhibit a high degree of orientation; it also contains amide groups with intermolecular hydrogen bonds that are stronger than is the intermolecular interaction in PET and PEN. As a result, ARAMID enables the formulation of high-strength, high-modulus films and are attractive for applications requiring ultrathin films with a high modulus. The glass transition temperatures, based on differential scanning calorimeter (DSC) measurement for PET, PEN, and ARAMID films, are typically reported as 80, 120, and 280°C, respectively.<sup>6,13</sup>

To study the effect of tape manufacturing on the properties of a substrate, two metal particle (MP) and two metal evaporated (ME) tapes that use PET and PEN substrates were used: MP-DLT [based on T-PET(2)], MP-LTO (based on T-PEN), ME-Hi8 [based on T-PET(3)], and ME-MDV [based on T-PEN(2)].<sup>11,12</sup> The substrates were obtained by carefully removing the front coat and back coat from the tape. The never-coated virgin substrate films were tested to compare them with the substrate to evaluate the degradation after tape manufacturing.

## Experimental apparatus and procedure

### Tensile tests

Tensile measurements were made using an MTS (MTS Systems Corp., MN) Model 804 tensile machine with a 50-lb load cell manufactured by Sensotech.<sup>17</sup> The tests were conducted at ambient temperature (19–22°C) and uncontrolled humidity (25–35% RH). According to the ASTM D 882-97 standard, rectangular 150  $\times$  10-mm-long samples with a grips' distance of 100 mm were selected to measure the Young's modulus (modulus of elasticity), F5 value (the stress at 5% elongation), strain at yield, breaking strength, and strain at break. The Young's modulus of all the samples was measured at the strain rate of 0.1/min. For the properties other than the Young's modulus, according to this standard, a strain rate of 0.1/min should be used if the strain at break of the specimen is lower than about 20% and a rate of 0.5/min should be used if the strain at break is 20–100%. Based on this recommendation, the selected strain rate was 0.1/min for ARAMID and 0.5/min for the other samples. Incidentally, as the breaking strength and yield strength may vary according to the sample geometry and test conditions, the F5 value is proven to be stable and independent and is commonly used in industry as the representative of mechanical strength for polymers. Polymeric films were tested in both the MD and the TD. A minimum of five tests was performed for each sample. The reproducibility of the data was within

about 5% for the Young's modulus and F5 value and about 10% for strain at yield, breaking strength, and strain at break.

#### DMA tests

A Rheometrics (Piscataway, NJ) RSA II dynamic mechanical analyzer was used to measure the dynamic mechanical properties of the polymeric films.<sup>1,7</sup> The analyzer was used in an autotension mode with a static force (about a 0.25% strain in this study) on the samples to prevent the thin films from buckling during application of the dynamic strain. Rectangular 22.5 × 6.35-mm samples were used. In this mode, a sinusoidal strain is applied to the specimen, and the corresponding sinusoidal load on the sample is measured by a load cell. Since the polymeric films are viscoelastic, there will be a phase lag between the applied strain and the measured load (or stress) on the specimen. The storage modulus,  $E'$ , is, therefore, a measure of the component of the complex modulus which is in-phase with the applied strain, and the loss modulus,  $E''$ , is a measure of the component which is out-of-phase with the applied strain. The in-phase stress and strain results in elastically stored energy which is completely recoverable, whereas out-of-phase stress and strain results in the dissipation of energy which is nonrecoverable and lost to the system. The loss tangent,  $\tan \delta$ , is simply the ratio of the loss modulus to the storage modulus.<sup>1</sup> Details of the procedure were described in ref. 7.

Frequency/temperature sweep experiments were performed for a 0.1–182 rad s<sup>-1</sup> (0.016–28 Hz) range, and 14 data points were taken for each frequency sweep at 11 different temperature levels ranging from -50 to 150°C for the PET films and 14 temperature levels ranging from -50 to 210°C for PEN films and ARAMID film. The temperature increment was 20°C, and the soak time for each temperature level was 10 s. For PET and PEN films, the upper limits for the test temperatures were set to cover the peak temperatures for the loss tangent related to the glass transition temperatures.

#### Longitudinal creep and shrinkage tests

Short-term creep, long-term creep, and shrinkage characteristics of polymeric films were evaluated using the test apparatus shown in Figure 2.<sup>6</sup> The apparatus is placed in an environmental chamber to measure the properties of interest at elevated temperature and/or humidity levels. The apparatus consists of four load beams (only one is schematically shown in Fig. 2) placed on a knife edge; by using four beams, four samples can be measured at a time. The film sample is vertically attached between one end of the load beam and the base. The load beam is adjusted on

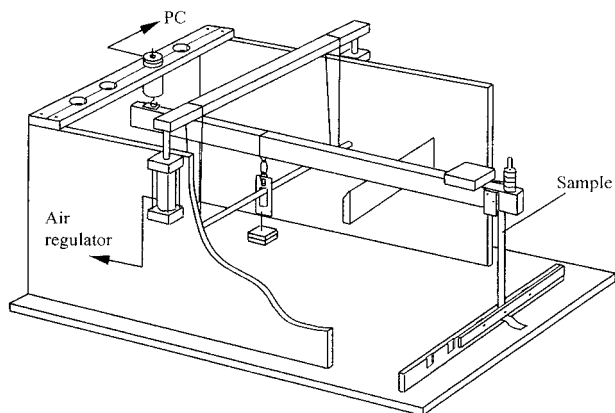
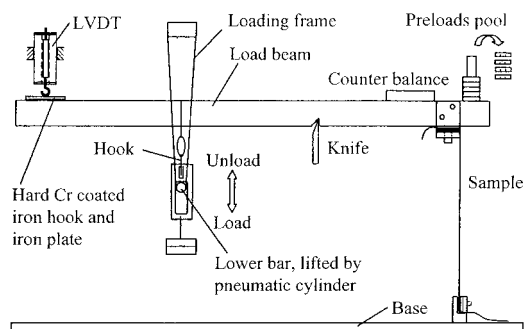


Figure 2 Schematic of creep and shrinkage test apparatus.

the knife in lateral direction to keep the sample straight in the vertical direction. A linear variable differential transformer (LVDT) is connected to the other end of the load beam to measure deflection due to the creep deformation of the film sample, and the output is recorded on a personal computer (PC). The load is applied on the load arm remotely using a pneumatically controlled mechanism, since the apparatus is placed in an environmental chamber. The dead weight is attached to a ring which is connected to a hook placed on the load beam. The ring is moved up or down in the vertical direction by moving the loading frame pneumatically, so that the hook is released or engaged and the dead weight is removed from or applied to the load beam, respectively. A counterbalance load is applied near the sample end in order to have no load on the sample before a desired load is attached. Load experienced by the sample is calibrated by placing weight on the load beam at the sample clamp region while the load beam is flat, for a range of loads on the other end. The LVDT reading is also calibrated by directly measuring the displacement at the sample end using a micrometer gauge and comparing it to the LVDT reading.

The samples were cut into 190 × 12.7-mm (1/2-in.) strips to accommodate the creep apparatus. The resulting strain was determined by measuring the

change in length of the samples relative to their original length. Prior to attaching the samples, the environmental chamber was turned on to stabilize the temperature and humidity and to allow the creep test apparatus to be conditioned for 1 h. The samples were then attached and conditioned at a preset temperature without any load for 1 h. Next, a preload of 0.5 MPa was applied to the samples by removing the corresponding weight from the preloads pool, and then the samples were conditioned for stabilization in an environmental condition. During this stabilization period of typically 2 h, the output signals were monitored until they were steady. The conditioning procedure, for instance, has the effect on the creep behavior of that the sample has lost its long-term memory and currently remembers loads applied in its immediate past history.<sup>14</sup> All creep tests were performed at a constant load of 7 MPa. This stress value was chosen because it is a typical stress applied to tapes in tape drives during use and has been shown to keep the creep deformation in the linear viscoelastic regime.<sup>1</sup> Since 55°C is the upper limit of the operating envelope for magnetic tapes, the maximum temperature used for the creep experiments was 55°C. The short-term creep measurements were performed at 25 and 55°C, with uncontrolled humidity (correspondingly 45–55% RH and 5–10% RH at 25 and 55°C) for the duration of 10, 30, 60, and 300 s. Then, the 7-MPa load was removed, and the samples were allowed to recover for a same period of loading. The long-term creep measurements were performed at 25, 40, and 55°C for a duration of 100 h, with uncontrolled humidity (50–60% RH, 15 to 25% RH, and 5 to 10% RH, respectively). In addition, to study the effect of the humidity, creep deformation under a severe condition was measured at 55°C and a controlled 80% RH. Creep measurements were made in the MD of the films, since stress is applied along the MD direction during operation and in a wound reel for a magnetic tape, which corresponds to the MD of the substrate films.<sup>6</sup> Shrinkage experiments were also performed at 55°C, 5–10% RH, and 55°C, 80% RH for 100 h, and a minimal applied stress of 0.5 MPa was used to hold the samples in place without causing any substantial creep for the samples. Shrinkage measurements were made both in the MD and in the TD.

#### Poisson's ratio, lateral creep, and CHE

The Poisson's ratio, long-term lateral creep, and CHE were measured by an LSM technique developed in the authors' group.<sup>8</sup> A laser scan micrometer system (transmitter, LS5041T; receiver, LS5041R; and controller, LS5501, from the Keyence Corp., Osaka, Japan) with an absolute measuring accuracy of about 2  $\mu\text{m}$  and resolution of 0.05  $\mu\text{m}$  was used to measure the changes in the width of the sample. In the technique,

the measurement of the change in width is important, and its relative accuracy is about  $\pm 0.1 \mu\text{m}$ . Polymeric films were sputter-coated with about a 5-nm-thick gold coating, so that they were opaque and could be measured by the laser beam. An opaque sample, 280  $\times$  12.7 mm, wrapped over a curved quartz glass, was loaded at 7 MPa on one end and fixed to a microgauge at another end; the laser scanning position on the sample was about 100 mm away from the fixed end. The experimental apparatus was placed inside a chamber where temperature and humidity are controlled within  $\pm 1^\circ\text{C}$  and  $\pm 2\%$  RH, respectively. After the temperature and humidity reach the expected values, the sample was conditioned for another 30 min before the test was started.

For the measurement of the Poisson's ratio, the sample was loaded in steps over a load range, say from 5 to 42 MPa at a step interval of 7 MPa. At each load level, the sample was held for 12 min to stabilize the measurement. The width profile was measured by moving the sample in the longitudinal direction at a speed of 10  $\mu\text{m}/\text{s}$ . By comparing the profiles at different load levels and matching the position of the characteristic features, the lateral and longitudinal displacements of the sample at the corresponding stresses were obtained. Thus, the longitudinal and lateral deformation and, consequently, the Poisson's ratio were calculated as follows:

$$\nu = \frac{\varepsilon_{\perp}}{\varepsilon_{\parallel}} = \frac{\Delta w/w}{\Delta l/l} = \frac{\Delta w l}{\Delta l w} \quad (1)$$

where  $\nu$  is the Poisson's ratio;  $\varepsilon_{\perp}$  and  $\varepsilon_{\parallel}$ , the lateral contraction and longitudinal elongation, respectively;  $w$  and  $\Delta w$ , the sample width and the decrease of the width, respectively; and  $l$  and  $\Delta l$ , the sample length from the microgauge to the measuring point and the increase of the length, respectively. Details of the technique can be found in refs. 8 and 11.

For measurement of the long-term lateral creep behavior, the sample was conditioned at 0.5 MPa for 1 h and loaded at another 7 MPa for 50 h. The width profiles were measured at various time periods. By comparing the profiles and matching the position of the characteristic features, the lateral contraction and longitudinal elongation at various times were recorded. For both the Poisson's ratio and the long-term lateral creep measurement, the nominal test conditions were set as 25°C, 50% RH. To study the effect of the humidity, tests at two conditions, 25°C, 15% RH, and 25°C, 80% RH, were conducted. To study the effect of the temperature, tests at 40°C, 50% RH, were conducted.

There is no corresponding ASTM standard for measuring the CHE for polymeric film. The most commonly used method is according to the Technical As-

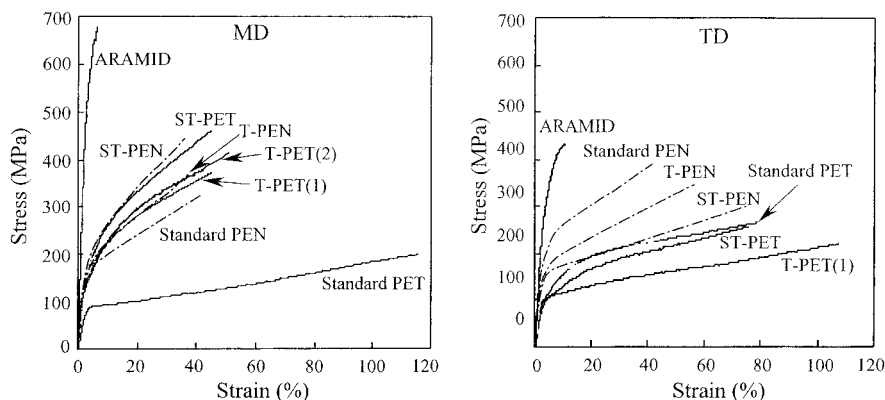


**Figure 3** Engineering stress-strain curves of various polymeric films. Strain rate for PETs and PENs was 0.5/min; strain rate for ARAMID was 0.1/min.

sociation of the Pulp and Paper Industry (TAPPI) Useful Method 549, for example, using a Neenah Multiple Specimen Paper Expansimeter (Adirondack Machine Corp., NY).<sup>1</sup> The typical reading accuracy for this expansimeter is  $\pm 13 \mu\text{m}$ , over a sample size of 127 mm (to 254 mm), which converts to a relative accuracy of  $\pm 10^{-4}$  for the measurement. The LSM technique has an extremely high accuracy,  $\pm 0.1 \mu\text{m}$  for a typical sample size of 12.7 mm (to 40 mm of accurate scanning range), which corresponds to a  $\pm 10^{-5}$  relative accuracy for the measurement, which is higher than that of the expansimeter method.

For CHE measurements, a  $42 \times 12.7$ -mm sample was slightly loaded in the longitudinal direction, and the dimensional change in the lateral direction was measured as the humidity changes from 20–80% RH, while the temperature is controlled at  $25 \pm 0.5^\circ\text{C}$ . The load is about 50 kPa, within the range recommended by ASTM E831-93 and D696-98 standards (for CTE measurement)<sup>15</sup> and is not supposed to result in significant longitudinal or lateral creep of the sample during the test. The reproducibility of the technique was found to be within  $0.5 \times 10^{-6}/\%$  RH. Two hygroscopic cycles were carried out on each sample.

#### Thermal expansion tests

The LSM apparatus was also used to measure the CTE. However, the temperature range limited by the LSM is below  $45^\circ\text{C}$ . Over such a small temperature range, the measurement error should be large and does not provide reliable data. Instead, a commercially available standard thermomechanical analyzer (TMA), a TA2940 (TA Instruments, USA), is commonly used and was used in this study to measure the CTE. In this instrument, the sample is mounted between a static stage and a floating probe. The dimensional change of the sample during heating is measured using an LVDT.<sup>11</sup> The typical sample size in this study is  $40 \times 3$  mm; after clipping, the gauge length of

the sample is approximately 25.5 mm. The temperature ranged from  $10^\circ\text{C}$  (precooled) to  $70^\circ\text{C}$ , at a heating rate of  $3^\circ\text{C}/\text{min}$ . A constant 3-g force was applied to the sample to keep it flat and stable. After the dimensional change of the sample was measured by an LVDT, it was converted to the CTE as

$$\alpha = \frac{\Delta l}{l \Delta T} \quad (2)$$

where  $\Delta l$  and  $l$  are the length change and the original length at  $10^\circ\text{C}$ , respectively, and  $\Delta T$  is the temperature range. According to ASTM E831-93, the measured CTE during the first  $20^\circ\text{C}$  of the test ( $10$ – $30^\circ\text{C}$ ) was regarded as unstable and was not used in the discussion in this study. A  $15.4$ - $\mu\text{m}$ -thick aluminum foil (Reynolds, OH;  $\text{CTE} = 23.6 \times 10^{-6}/^\circ\text{C}$ ) was used to calibrate the instrument. The results of three repeated tests on this foil were  $23.6$ ,  $23.4$ , and  $23.6 \times 10^{-6}/^\circ\text{C}$ . So, the TMA was proven to have a good repeatability.

The CTE in the thickness direction of the polymeric films were measured by Teijin-DuPont Co. (Japan) and Ulvac-Riko (Japan).<sup>16</sup> In this technique, the sample is mounted between two optical transparent spacers. A laser interference technique is used to measure the thickness change of the sample while temperature is changed. Ten layers of film were piled together to get a  $50$ - $\mu\text{m}$ -thick sample to obtain good results.

## RESULTS AND DISCUSSION

### Tensile tests

The engineering stress-strain curves of various films along the MD and the TD are shown in Figure 3.<sup>7</sup> All the samples deformed uniformly during the test, and no necking was formed. The Young's modulus ( $E$ ), F5 value (stress at 5% strain), breaking strength ( $\sigma_b$ ), strain at yield ( $\epsilon_y$ ), and strain at break ( $\epsilon_b$ ) are summarized in Table II. Comparing the properties of stan-

TABLE II  
Tensile and DMA data

Sample		Tensile test data					DMA test data			
		E (GPa)	F5 (MPa)	$\varepsilon_y$ (%)	$\sigma_b$ (MPa)	$\varepsilon_b$ (%)	$E'$ (GPa) at 25°C		$E'$ (GPa) at 50°C	
							0.016 Hz	28 Hz	0.016 Hz	28 Hz
Standard PET	MAJ	3.30	95	3.00	200	115	4.08	4.25	3.84	4.05
	MIN	4.54	117	4.10	266	79	5.01	5.33	4.67	5.04
T-PET(1)	MD	6.30	172	3.10	350	44	6.29	6.73	5.92	6.45
	TD	4.10	106	2.80	230	108	4.16	4.45	3.91	4.20
T-PET(2)	MD	7.45	166	3.20	414	51	7.11	7.65	6.54	7.16
	TD	4.90	109	2.00			4.43	4.74	4.16	4.51
ST-PET	MD	7.15	195	3.30	461	45	7.34	7.88	6.91	7.38
	TD	4.47	107	3.20	257	75	4.57	4.90	4.43	4.61
Standard PEN	MD	6.25	175	3.20	334	42	6.18	7.92	4.93	6.85
	TD	6.90	200	3.20	384	42	6.46	8.30	5.18	7.16
T-PEN	MD	6.50	190	2.60	340	30	6.82	9.11	5.37	7.85
	TD	5.60	158	2.90	300	40	6.18	7.92	4.93	6.85
ST-PEN	MD	7.80	220	2.70	452	36	7.53	9.75	6.08	8.47
	TD	5.42	144	2.65	293	75	5.11	6.61	3.96	5.73
ARAMID	MD	20.4	628	2.80	638	6.4	16.95	21.03	15.4	19.9
	TD	11.3	338	3.80	433	11	11.1	14.6	10.7	14.8

dard and tensilized films, it can be seen that tensilization significantly increases the Young's modulus, F5 value, and breaking strength of the PET and PEN films in the MD. For example, the Young's modulus of standard PET (3.3 GPa) is doubled after tensilization [T-PET(1): 6.3 GPa] and supertensilization (ST-PET: 7.4 GPa). But the deformation properties—strain at break and strain at yield—are decreased after tensilization. These tendencies reverse in the TD, as the Young's modulus changes from 4.5 GPa for standard PET to 4.1 GPa for T-PET(1) and the strain at break changes from 79% for standard PET to 108% for T-PET(1).

Standard PET shows a fairly low work-hardening ratio ( $d\sigma/d\varepsilon$ ) after the elastic limit is reached in the MD, while T-PET(1) and (2) and ST-PET have relatively high work-hardening ratios. The increase in the hardening ratio as a result of tensilization arises since the chain segments in the amorphous regions are extended in a variety of degrees. In other words, tensilized films contain more oriented chains than do standard films, which effectively restrain the molecular deformation along the drawing direction.

Tensilization has similar effects on PEN films as on PET films, but is not that significant. For example, the modulus for standard PEN increases from 6.2 to 6.5 GPa (T-PEN) and 7.8 GPa (ST-PEN) in the MD and decreases from 6.9 to 5.6 GPa (T-PEN) and 5.4 GPa (ST-PEN) in the TD after tensilization.

ARAMID exhibits a high Young's modulus and strength and low elongation, and it is more anisotropic than are PET and PEN films. The Young's modulus

along the MD and the TD are 20.4 and 11.3 GPa, respectively, as compared to 9.5 GPa (MD) and 10.5 GPa (TD) in a previous article by Ezquerro et al.<sup>17</sup> This is probably due to an improvement in tensilization along the MD during the manufacturing process.

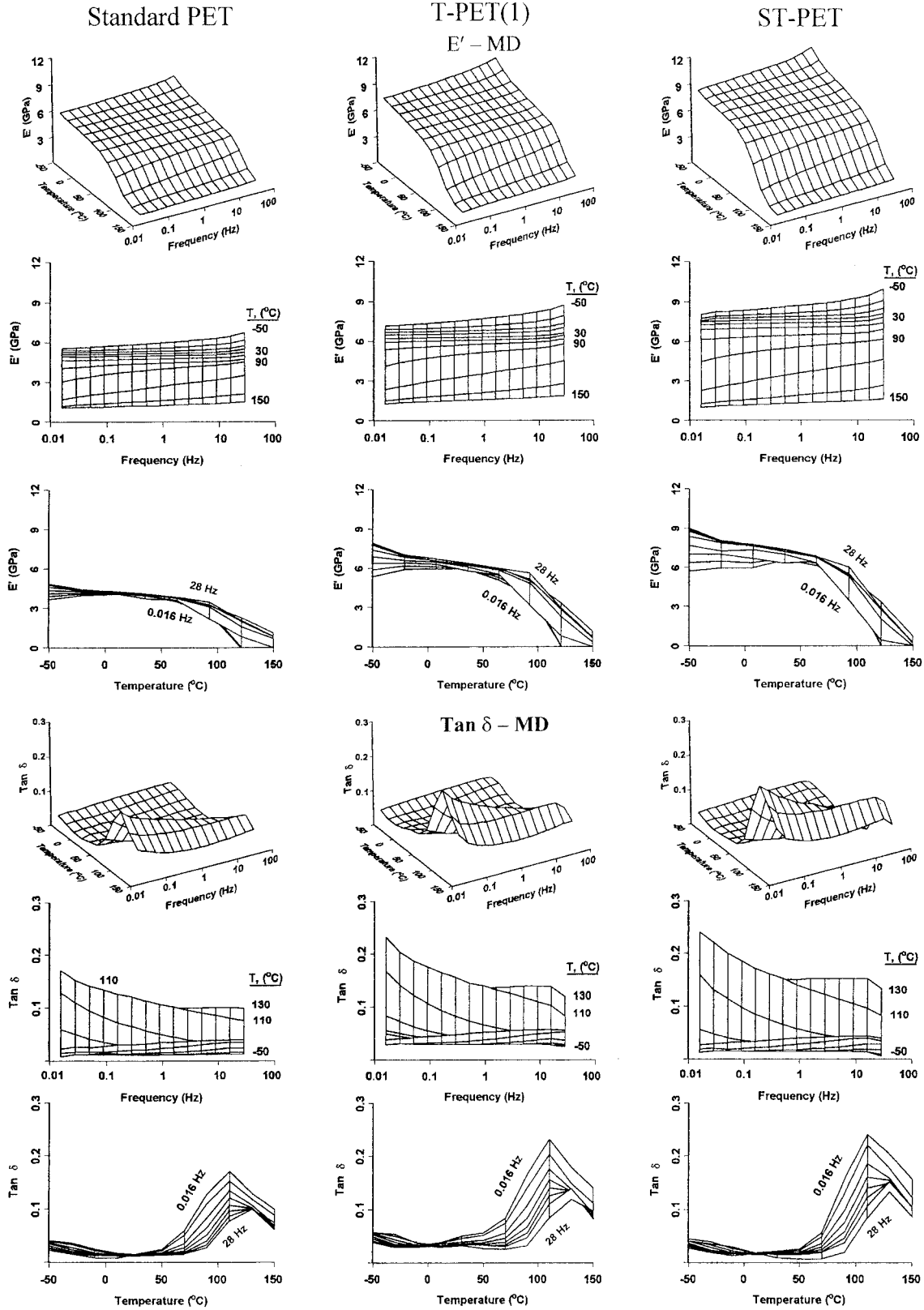
### Dynamic mechanical analysis (DMA)

#### DMA data

Examples of the results from the DMA for various polymeric films are shown in Figure 4.<sup>7</sup> Figure 4(a) shows the storage moduli and loss tangent of standard PET, T-PET(1), and ST-PET in the MD. Figure 4(b) shows a comparison of DMA data for various kinds of materials in the MD.<sup>7</sup> For the sake of saving space, we do not present all the data for all three PEN films. There are some common points among the PET and PEN films: The storage modulus increases as the frequency increases and the temperature decreases. There is a major peak at the loss tangent–temperature curve, which corresponds to the glass transition temperature. Above this temperature, the polymeric material behaves as a viscoelastic rubber due to the rotation of the molecular backbone, such as the —O— bond. The glass transition temperatures for PET and PEN films defined by the peak temperature of the loss tangent are 110–130 and 140–170°C at 0.016 and 28 Hz, respectively.

The temperature at which the peak of the loss tangent occurs is a function of frequency<sup>18</sup>; it shifts to a lower value and higher temperature as the frequency

Effect of tensilization on PET films

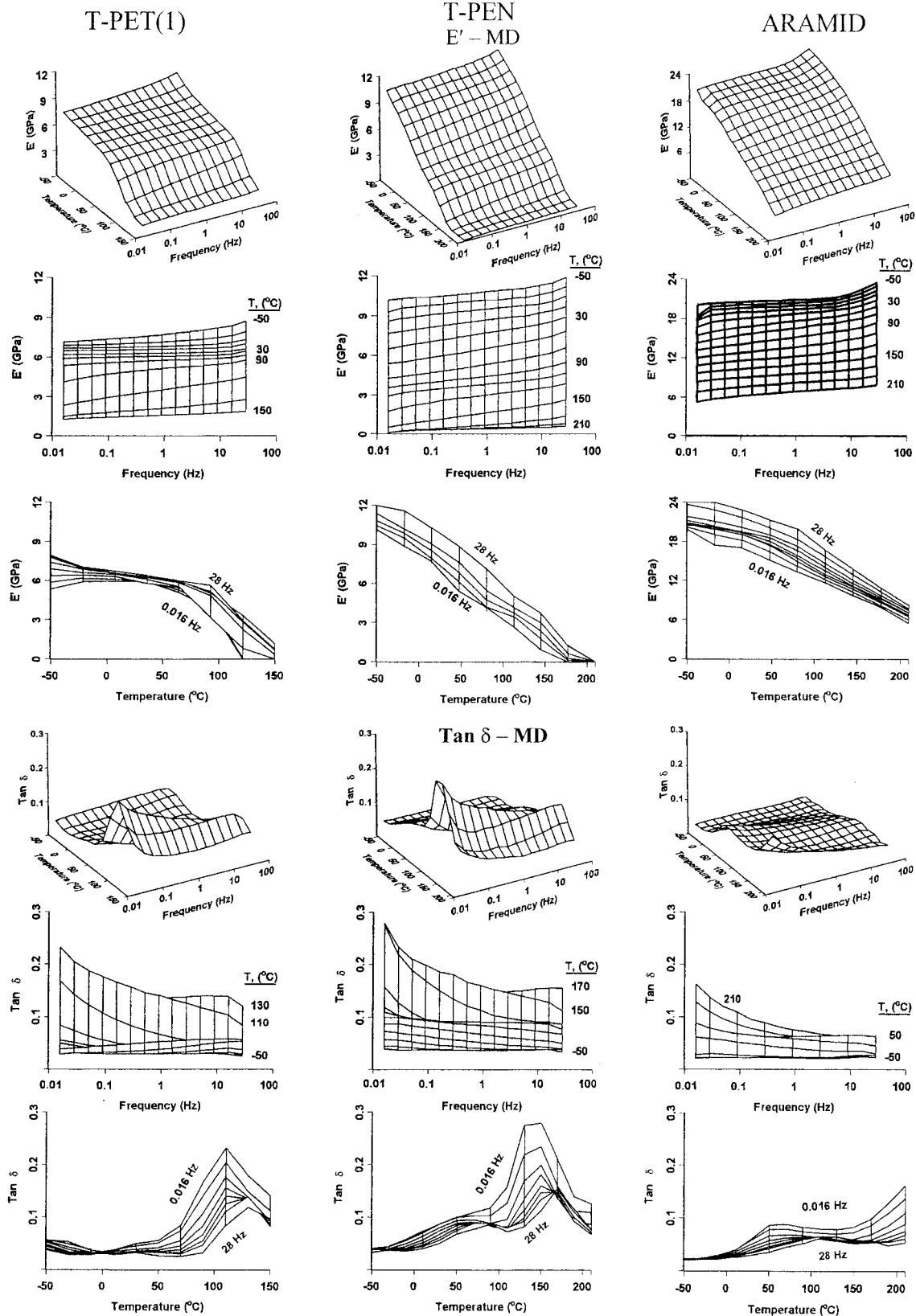


(a)

Figure 4 DMA data: storage modulus and loss tangent in the MD, showing (a) the effect of tensilization on PET films and (b) films of various materials.



Films of various materials



(b)

Figure 4 (Continued from the previous page)

increases, due to the frequency dependence of the relaxation processes. For example, the loss tangent peak for standard PET shifts from 0.22 at 110°C to 0.12 at 130°C as the deformation frequency increases from 0.016 to 28 Hz. Essentially, the faster the applied stimulus, the less time the molecules have to respond to it; therefore, a high temperature is needed to energize molecular movement at high frequencies. On the other hand, at a constant temperature, as the stimuli are applied over a range of frequencies, the glass transition is seen first for the lower frequencies. Minimal movement of the molecular chain at high frequencies also explains the continuous decrease in the loss tangent as the frequency increases. From the frequency dependence of the loss tangent peak, it is possible to evaluate the activation energy for the process.<sup>18</sup>

The long-range molecular motion at the glass transition temperature is less affected by the molecular orientation. As presented in Figure 4(a), the loss tangent peaks' temperature is slightly affected by tensilization.<sup>7</sup> But tensilized films have higher peak values of the loss tangent than those of standard films. The loss tangent is a factor indicating the ratio of unrecoverable dissipated energy over recoverable elastic energy during the deformation. One of the differences between standard and tensilized films is that there is more residual stress in the later ones. This residual stress was built up during the drawing at elevated temperature during the manufacturing, usually around the glass transition temperature. The films were then thermal set or annealed at a temperature below the glass transition temperature (or very shortly exposed to a temperature higher than the glass transition temperature) to relax most of the internal stress, but, unavoidably, some internal stress was left in the final film and is called residual stress. This residual stress can be effectively relaxed only at the temperature around the glass transition temperature or above. The relaxation of the residual stress during the test results in extra unrecoverable deformation, or unrecoverable energy, and was reflected by a high loss tangent in the DMA tests.

Besides the glass transition temperature, there are some other differences between the properties of PET and PEN films. In comparing the storage modulus versus temperature figures for T-PET(1) and T-PEN, the distance between the curve at 0.016 Hz and the curve at 28 Hz for T-PEN is larger than that for T-PET(1), meaning that PEN films have a higher frequency dependence as compared to the PET films. Unlike the PET films of which the storage modulus remains almost constant at the glassy state, the storage modulus of PEN films decreases with a certain slope in the whole temperature range. A high rate of decrease of the storage modulus of PEN films corresponds to a high value of the loss tangent. The effect of tensilization on the peak value of the loss tangent for

the PEN films was not that obvious as that for the PET films. The values for standard PEN, T-PEN, and ST-PEN are 0.27, 0.25, and 0.26, respectively, compared to 0.17, 0.23, and 0.24 for standard PET, T-PET(1), and ST-PET, respectively. Similar values may indicate that the magnitude of residual stresses in these PEN films are of similar order. Also, for PEN films, there is a minor loss tangent peak at 20–70°C (called  $\beta^*$  relaxation) in addition to the peak that is related to the glass transition at 140–170°C (called  $\alpha$  relaxation). This peak was absent for PET films. The origin of this  $\beta^*$  relaxation in PEN film was conjectured to be due to the motion involving interlayer slippage among the naphthalate segments.<sup>19</sup> Due to the limitation of the test temperature range, a minor peak at about -70°C was not observed for either the PET or PEN films,<sup>13</sup> which corresponds to the localized motion of the —COO— groups in PET and PEN molecules. This relaxation is called the  $\beta$  relaxation, or the secondary relaxation, distinguished from the  $\alpha$ , or primary relaxation, at the glass transition temperature.<sup>13,18</sup>

ARAMID has a significantly higher storage modulus than those of PET and PEN films. It also has good temperature resistance; for example, the storage moduli remains above 6 GPa even at 200°C in both the MD and the TD. The glass transition temperature for ARAMID is typically reported as 280°C according to the DSC test, so there is no glass transition peak in the loss tangent–temperature diagram in this study; instead, only a steady increase is present in the 170–210°C range. But like the curves of PEN films, a minor loss tangent peak at 50°C (at 0.016 Hz) to 130°C (at 29 Hz) is present, which is responsible for the decrease in the storage modulus near this temperature.

Figure 5 shows the effects of the frequency and temperature on the DMA properties of various polymeric films along the MD at 30°C and 0.16 Hz, respectively, so that we can have a general comparison with different films. ARAMID has the highest storage modulus among the films. The storage moduli for PEN films are higher than those for PET films, but the difference is reduced as the deformation frequency decreases during the test. In general, the storage modulus at higher frequency is determined mainly by the elastic elements, and it is the viscoelastic properties—like creep deformation—that predominate the storage modulus at lower frequency. The storage moduli of the same material (such as standard PET, T-PET, and ST-PET) have similar slopes against frequency and temperature.

#### Prediction of mechanical behavior using time–temperature superposition

A technique known as time–temperature superposition was used to predict the storage moduli over a wider frequency range at a specific reference temper-

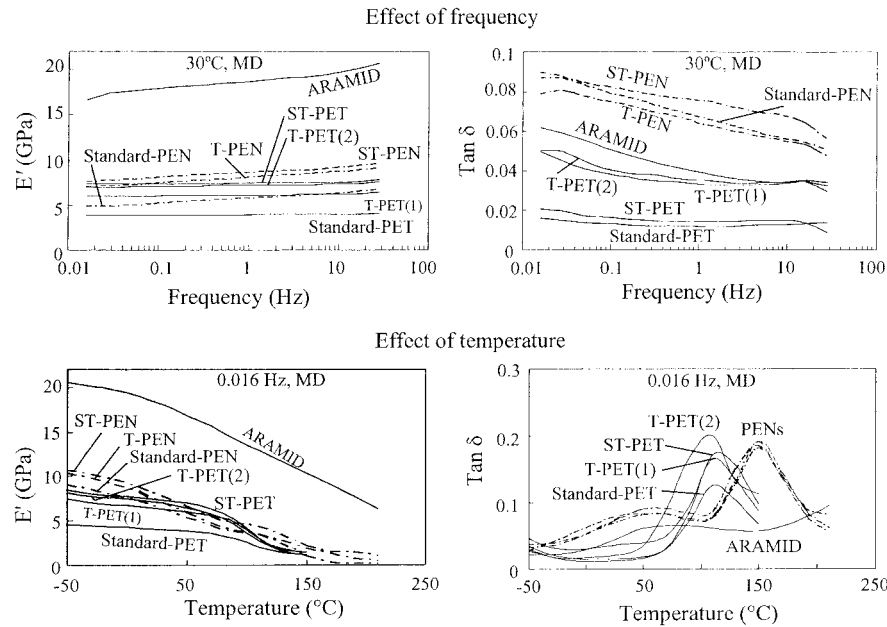


**Figure 5** Effects of frequency (at 30°C) and temperature (at 0.016 Hz) on storage modulus and loss tangent in the MD for various polymeric films.

ature.<sup>1,14,20–22</sup> The superposition was carried out using DMA data taken over a relatively narrow frequency range at different temperature levels.<sup>7</sup> For instance, the storage modulus versus frequency curves in Figure 4(a) were used as the starting point, and a reference temperature of 30°C was selected. In a logarithmic scale, curves at temperatures higher than 30°C were shifted to the left until they fit together smoothly, and the curves corresponding to the temperatures lower than 30°C were shifted to the right. The shift direction corresponds to the visoelastic nature of polymeric films. Storage moduli measured for a polymer at high

frequencies under ambient conditions would be equivalent to those measured at lower frequencies and temperatures.

Based on the time–temperature superposition, master curves were generated. Two plots are shown in the MD and the TD in Figure 6. The results are shown on a log–log scale and indicate the storage modulus along the MD and the TD over a frequency range from  $10^{-20}$  to  $10^{10}$  Hz. The storage modulus curves for PET and PEN films can be identified as two regions according to the slopes separated at about  $10^{-10}$  Hz (PET films) and  $10^{-7}$  Hz (PEN films), respectively. As a matter of

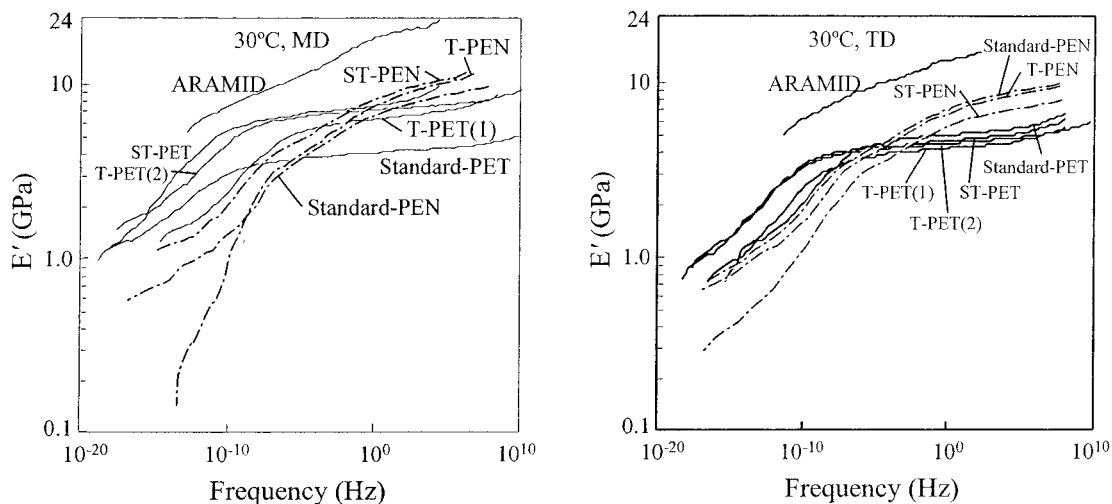


**Figure 6** Master curves of storage modulus for various polymeric films at 30°C.

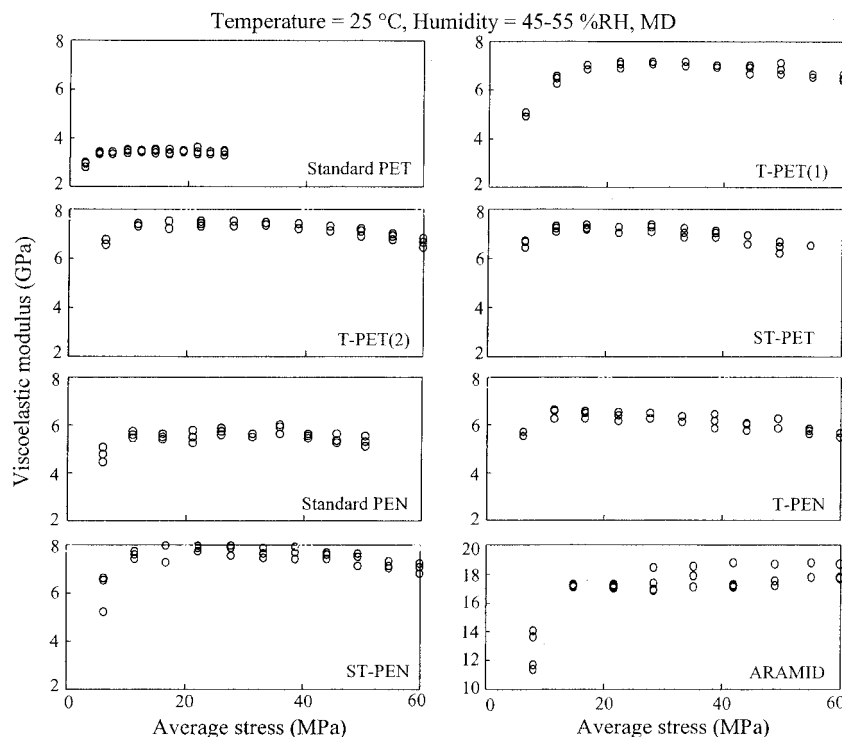


**Figure 7** Viscoelastic moduli for some polymeric films as a function of average stress at 25°C, 45–55% RH. The loading period is 15 s.

fact, the storage modulus data for PET at frequencies lower than  $10^{-10}$  Hz come from the storage moduli at temperatures higher than the glass transition temperature. Thus, the curves can be regarded as composed of a glassy region and a rubbery region. When the deformation frequency is lower than  $10^{-10}$  Hz (317 years), PET films will behave as a rubber and PEN films will behave as a rubber when the deformation frequency is lower than  $10^{-7}$  Hz (4 months). PEN films appear to be stiffer than are PET films at frequencies higher than  $10^{-2}$  Hz (for the MD) and  $10^{-6}$  Hz (for the TD); when the deformation frequencies are lower than that, the storage moduli for PET films are higher than those for PEN films. Tensilization shifts the storage modulus curves for PET and PEN films to a higher value, and this effect is more obvious for PET films. Tensilization also shifts the cross frequency toward higher frequencies. But tensilization does not affect the threshold frequencies for the transition from glassy to rubbery.

ARAMID, over the available frequency range ( $10^{-10}$  to  $10^5$  Hz), has a superior storage modulus compared to other polymeric films, although the decreasing rate of the storage modulus as a function of the frequency is relatively high. There is no glass transition for ARAMID in the frequency range corresponding to the temperature range used in this study; the whole curve is within the glassy region.

### Longitudinal creep and shrinkage tests

Calibration and compensation of the experimental deformation at 7 MPa

During the longitudinal deformation tests, the strain in the 7 MPa stress range at the initial loading duration was not stable, which covers the so-called toe region in the engineering strain–stress curve (ASTM 882-97, ref.15). According to ASTM standards, the deformation of the sample in the low stress range, either loading or unloading, contains an artifact. It is an artifact caused by a take up of the slack and alignment or seating of the specimen, which does not represent a property of the material. To give a quantitative demonstration, we first define a term, viscoelastic modulus, as the stress amplitude divided by the strain amplitude over a period of loading, for example, 15 s, representing the combination of elastic and viscoelastic properties of the films. Viscoelastic moduli of all the polymeric films as a function of stress were measured at 25 and 55°C, using the longitudinal deformation test apparatus. Selected results at 25°C for the viscoelastic moduli are shown in Figure 7. Stable moduli were obtained only when the stress was higher than a certain value. Very careful sample mounting may reduce this value. In this study, the “toe” stress is about 5 MPa. So, the deformation of polymeric films from 0.5 to 7.5 MPa is not stable (0.5 MPa is the

preload), but the creep behavior of these films at 7.5 MPa falls into stable deformation region. For example, a T-PET(1) film sample shows a 0.20% elongation when it is loaded from 0.5 to 7.5 MPa at 55°C, 5–10% RH; then, at this constant stress, the elongation becomes 0.21% after 100 s. We believe that the elastic elongation, 0.20%, is not reasonable because it contains an artifact. But the creep elongation, 0.21% – 0.20% = 0.01%, is stable and represents the viscoelastic property of the film at 7.5 MPa and a duration of 100 s. A similar principle applies to the unloading.

In this study, we measured the viscoelastic property of the films at a stress range of 0.5–7.5 MPa. Then, we made a compensation to remove the effects of the toe region. This was achieved by applying the stable viscoelastic modulus to calculate the theoretical initial strain and creep compliance at a 7-MPa stress span.

To obtain the theoretical initial strain at a 7-MPa stress, 15 s, for the compensation to creep data (either short-term or long-term creep), the test conditions should be the same as for the creep test. Elastic moduli from the tensile test<sup>7</sup> cannot be used since the deformation speed (strain rate) is too high. In this study, we used the same apparatus and conditions to measure the viscoelastic moduli for polymeric films using the following steps:

The sample was preloaded at 5 MPa and conditioned for 0.5 h at a corresponding temperature and humidity. Then, an extra 7-MPa load was applied; the strain at 15 s was recorded to calculate the viscoelastic modulus of this sample at the stress range of 5–12 MPa and 15 s. These data were plotted as a viscoelastic modulus at an average stress of  $(5 + 12)/2 = 8.5$  MPa in Figure 7. The 7-MPa load was then removed and the sample was allowed to have a short period recovery (about 5 min). Then, it was preloaded at 10 MPa, conditioned for 0.5 h, and then an extra 7 MPa was applied. The strain at 15 s was measured and was used to calculate the viscoelastic modulus of this sample at the stress range of 10–17 MPa and 15 s. The data were plotted as a modulus at 13.5 MPa in Figure 7. This process was repeated at elevated preloads at 25°C, so the moduli as a function of stress were obtained, as shown in Figure 7. At 55°C, it is not necessary to measure the moduli across a large stress range, since the films are prone to creep more at high temperature, and the moduli correspondingly decrease at a high stress. In this case, the moduli at 0-, 5-, 10-, and 15-MPa preloads were measured. The stable moduli were also found to be at an average stress higher than 5 MPa.

At least three tests were performed on each film. The moduli at a stable stress range were then averaged to obtain the final viscoelastic modulus for each film at each temperature, and the data are listed in Table III.

The compensation of the “toe” in the loading region was achieved by applying the viscoelastic moduli and corresponding creep compliance ( $1/\text{viscoelastic mod-}$

**TABLE III**  
Viscoelastic Moduli and Creep Compliance of Polymeric Films at 15 s (MD)

Sample	25°C <sup>a</sup>		55°C <sup>b</sup>	
	<i>E</i> (GPa)	<i>D</i> (GPa <sup>-1</sup> )	<i>E</i> (GPa)	<i>D</i> (GPa <sup>-1</sup> )
Standard PET	3.33	0.300	3.21	0.312
T-PET(1)	6.66	0.150	6.01	0.166
T-PET(2)	7.10	0.141	6.26	0.160
ST-PET	7.20	0.139	6.50	0.154
Standard PEN	5.50	0.182	4.44	0.225
T-PEN	5.92	0.169	4.80	0.208
ST-PEN	7.25	0.138	6.23	0.161
ARAMID	17.54	0.057	14.41	0.069

<sup>a</sup> Stress range is 10–42 MPa.

<sup>b</sup> Stress range is 10–22 MPa.

ulus) in Table III. For example, Figure 8(a) schematically shows the raw data of the instantaneous creep curve of T-PET(1) at 55°C. From Table III, the viscoelastic modulus of T-PET(1) at 55°C is 6.01 GPa; correspondingly, the creep compliance at 15 s is the reciprocal of the viscoelastic modulus,  $1/6.01 = 0.166$  GPa<sup>-1</sup>. Thus, in Figure 8(b), the creep curve was shifted down to fit the point (15 s, 0.166 GPa<sup>-1</sup>). The relative position of the points in the creep curve does not change during the shifting.

Next, we address the artifacts during unloading. The recovery compensation is achieved by applying the fully recovery data. After the recovery that lasts 100 times that of the loading period, the sample is supposed to be fully recovered if the sample is linearly viscoelastic. This is regarded as the zero length to calibrate the recovery curves [as shown in Fig. 8(c)].

#### Short-term creep behavior

Figure 9(a,b) shows the short-term creep of the polymeric films at 25 and 55°C. These curves are obtained after correcting for extraneous deformations. The curves include short-term creep (10, 30, 60, and 300 s) and, correspondingly, recovery for the same period. For each film, curves of different creep periods show good reproducibility, which demonstrates that the test technique works well. The short-term creep compliance data at 10, 30, and 300 s are listed in Table IV.

Due to the sensitivity of the test system, the vibration of the samples at the first couple of seconds during the loading was also recorded (Fig. 9). Systematically, PET films show more oscillation than do PEN films. This may imply that PEN films have a better damping performance in handling during the tape manufacturing than have PET films.

Initial creep compliance is the creep compliance in the couple of seconds after loading. It is reflected by the viscoelastic modulus in this study. The elastic moduli and viscoelastic moduli are summarized in Tables II and III, respectively. The elastic moduli of

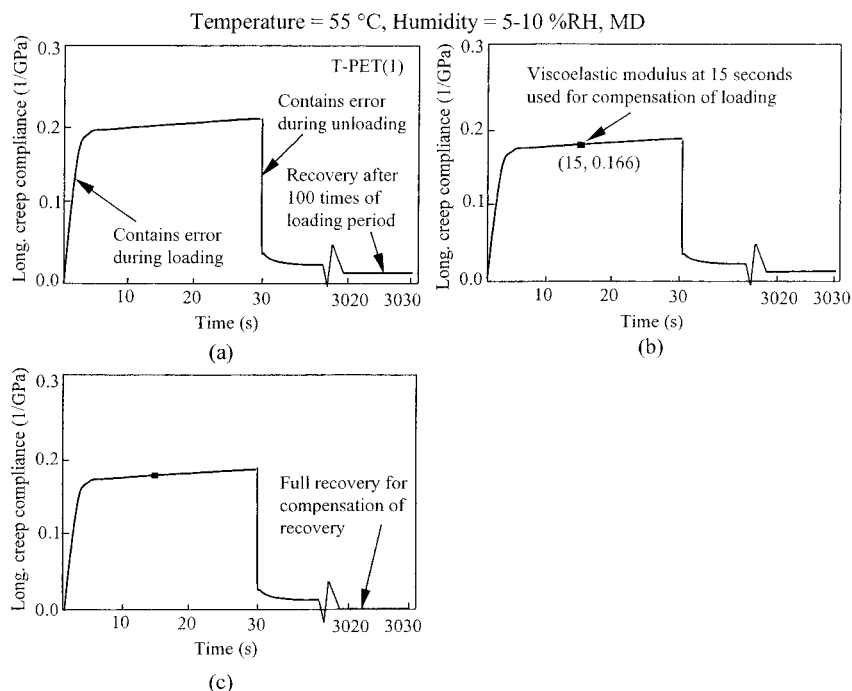


**Figure 8** Schematic diagrams of “toe” compensation: (a) raw data from short-term creep test; (b) compensation of loading; (c) compensation of recovery.

PEN films are generally higher than those of PET films; for example, the Young’s modulus at 25°C, 28 Hz, for T-PEN is 9.1 GPa and that for T-PET(1) and T-PET(2) are 6.7 and 7.6 GPa, respectively. This elucidates that the elastic stiffness of PEN films is higher than those of PET films. But, in Table III, the 15-s viscoelastic modulus (at 25°C) for T-PEN is 5.9 GPa, while that for T-PET(1) and T-PET(2) are 6.7 and 7.1 GPa, respectively. This means that PEN is superior to PET in elastic properties whereas it is inferior to PET in viscoelastic properties. The situation at 55°C is similar to that at 25°C.

The reason for the above phenomena, as discussed in ref. 7, is due to the different molecular structures of PET and PEN films. PEN has a naphthalene ring in its molecule, which is more elastically stiffer than is the benzene ring in the PET molecule. But PET films have a higher crystallinity (40–50%) than that of PEN films (30–40%). Note that molecular creep and relaxation occur only in the amorphous region; also, from the DMA data in refs. 7 and 13, PEN films have a  $\beta^*$  relaxation around room temperature. That is why PEN films show lower viscoelastic moduli at 25 and 55°C than those of tensilized PET films.

*Creep velocity.* The viscoelastic property of a polymer film may be more properly demonstrated by another parameter: creep velocity, which is the first derivative of creep compliance  $[D(t)]$  over time.<sup>23</sup> For a generalized Voigt–Kelvin model which consists of a group of Voigt–Kelvin elements in series (e.g., ref. 1),

$$D(t) = D_0 + \sum_{i=1}^n \{D_i [1 - \exp(-t/\tau_i)]\} \quad (3)$$

$$\frac{dD(t)}{dt} = \sum_{i=1}^n \left[ \frac{D_i}{\tau_i} \exp(-t/\tau_i) \right] \quad (4)$$

where  $D_0$  is the elastic compliance,  $D_i$  represents the creep compliance spectra at a time equal to zero when constant stress is applied, and  $\tau_i$  represents discrete spectra of retardation times which determine the rate of decay of the first derivative of  $D_i(t)$ .

The concept of creep velocity is more suitable to be discussed in short-term creep behavior, rather than in long-term creep behavior. As is well known, the tape substrate films are highly tensilized in the MD and the TD during the manufacturing, so that desired mechanical properties, such as a high young’s modulus along these directions, are obtained. Although the films are then thermal set, or annealed after drawing, the residual strain (or stress) cannot be thoroughly eliminated. The relaxation of this residual strain/stress is a viscoelastic behavior and results in shrinkage of the film. This viscoelastic process is time- and temperature-dependent. Elevated temperature accelerates this process by improving the mobility of the molecular segments. Since the samples were conditioned before the test, the effect of shrinkage was not obvious in the

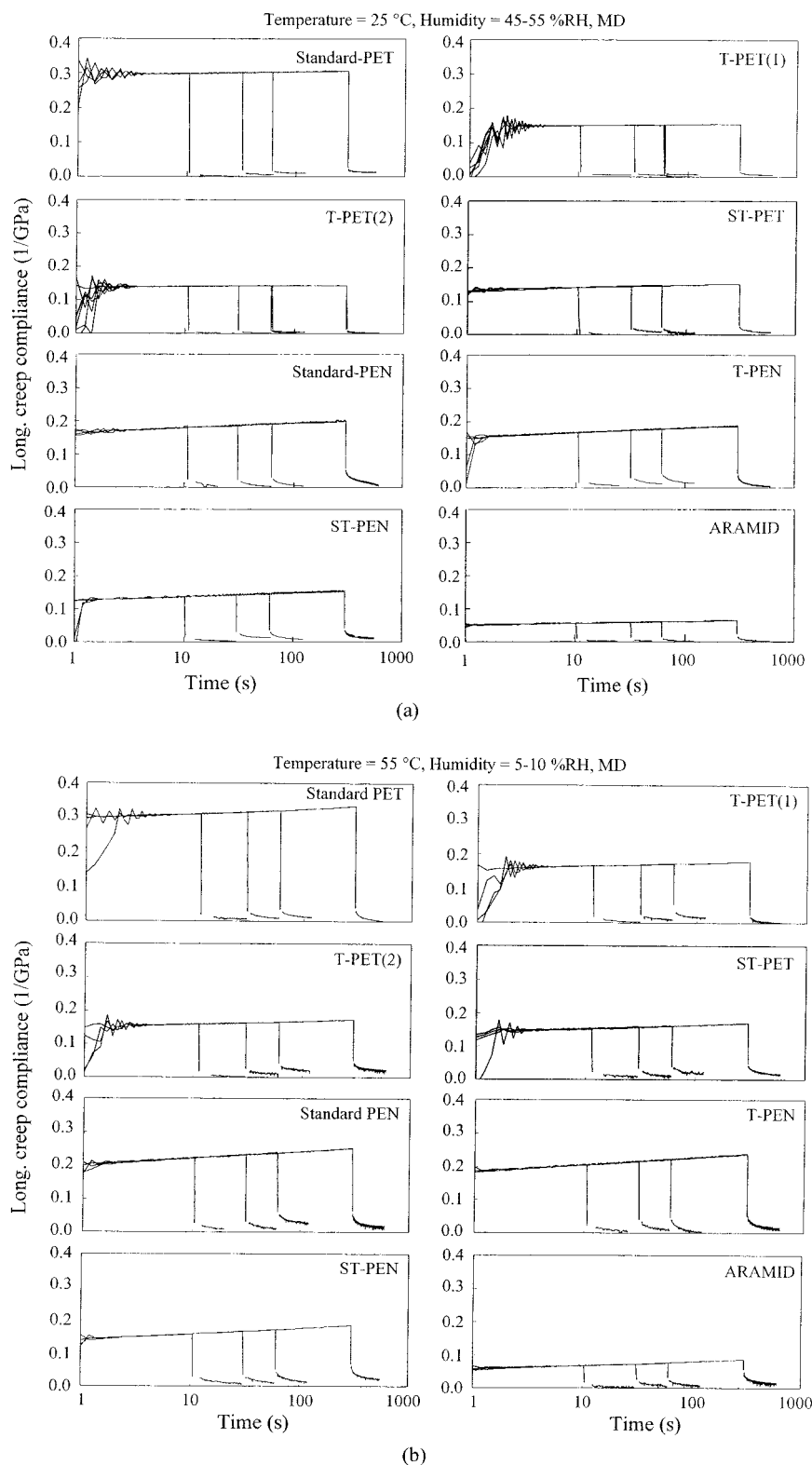


**Figure 9** Longitudinal short-term creep behavior of polymeric films at (a) 25°C, 45–55% RH, and (b) 55°C, 5–10% RH.

short-term creep test. But the shrinkage would be significant or even surpass the creep effect in the long-term creep test. Therefore, for the short-term creep behavior, creep velocity provides relevant information.

Figure 10 summarizes the 300-s creep compliance and 250-s recovery of polymeric films at 25 and 55°C, in linear and log scale. In the logarithmic figures, PEN films show significantly higher creep velocity than that of PET films. Figure 11 shows the creep velocities

**TABLE IV**  
**Short-term Longitudinal Creep Compliance ( $\text{GPa}^{-1}$ ) of Polymeric Films at a Stress of 7 MPa in MD**

Sample	25°C, 45–55% RH			55°C, 5–10% RH		
	10 s	30 s	300 s	10 s	30 s	300 s
Standard PET	0.300	0.302	0.307	0.311	0.316	0.334
T-PET(1)	0.150	0.151	0.154	0.165	0.168	0.177
T-PET(2)	0.141	0.142	0.145	0.159	0.163	0.174
ST-PET	0.139	0.141	0.143	0.153	0.157	0.169
Standard PEN	0.181	0.187	0.201	0.222	0.231	0.251
T-PEN	0.167	0.174	0.188	0.205	0.215	0.237
ST-PEN	0.136	0.142	0.153	0.158	0.166	0.185
ARAMID	0.057	0.059	0.064	0.067	0.073	0.087

of the polymeric films at 25 and 55°C. At both temperatures, trends of the creep velocities of films are similar: PEN films exhibit the highest velocity, followed by ARAMID and PET films; tensilized PET films exhibit the lowest velocity. The difference between that for tensilized PET and PEN films is about one decade. Referring to the DMA presented earlier,<sup>7</sup> the PEN films have a  $\beta^*$  relaxation at room temperature (20–70°C) in their loss tangent–temperature curves. Correspondingly, storage moduli of the PEN films show an obvious decrease across this tempera-

ture range. Together with the creep compliance data, we can draw the conclusion that, at a normal application temperature, PEN films show more viscoelasticity and creep acceleration than do PET films, especially tensilized PET films. ARAMID was also found to have a high loss tangent value around ambient temperature and a creep velocity higher than that of PET film but lower than that of PEN films. Since ARAMID film has a significantly higher young’s modulus than that of polyester films, its absolute deformation at the same test condition is the lowest among all the films in this study. At 55°C, the behavior of PEN films was still  $\beta^*$  relaxation-governed, while that for PET films was slightly  $\alpha$  relaxation-governed. This is reflected by that the difference of the creep velocity between PET and PEN films at 55°C was smaller than that at 25°C.

*Residual creep compliance and recovery.* In Figure 9, the initial residual creep compliance (the creep compliance at the first couple of seconds of recovery) of all the films increases as the loading period increases. For example, at 25°C, the 2-s residual creep compliance (2 s after unloading) of standard PET after 10 s creep is  $0.008 \text{ GPa}^{-1}$ ; after 30 s,  $0.02 \text{ GPa}^{-1}$ ; after 60 s,  $0.025 \text{ GPa}^{-1}$ ; and after 300 s,  $0.03 \text{ GPa}^{-1}$ . This corresponds to an increased residual strain after an increased loading period in the test.

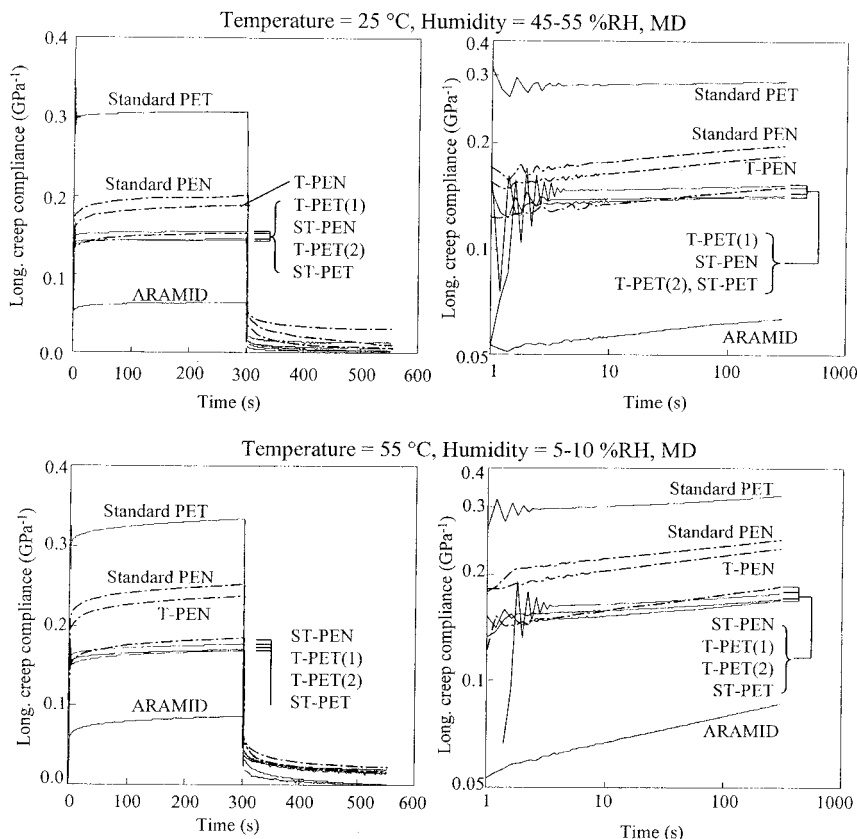


**Figure 10** Comparison of 300-s short-term creep behavior of polymeric films in the MD at 25°C, 45–55% RH, and 55°C, 5–10% RH.



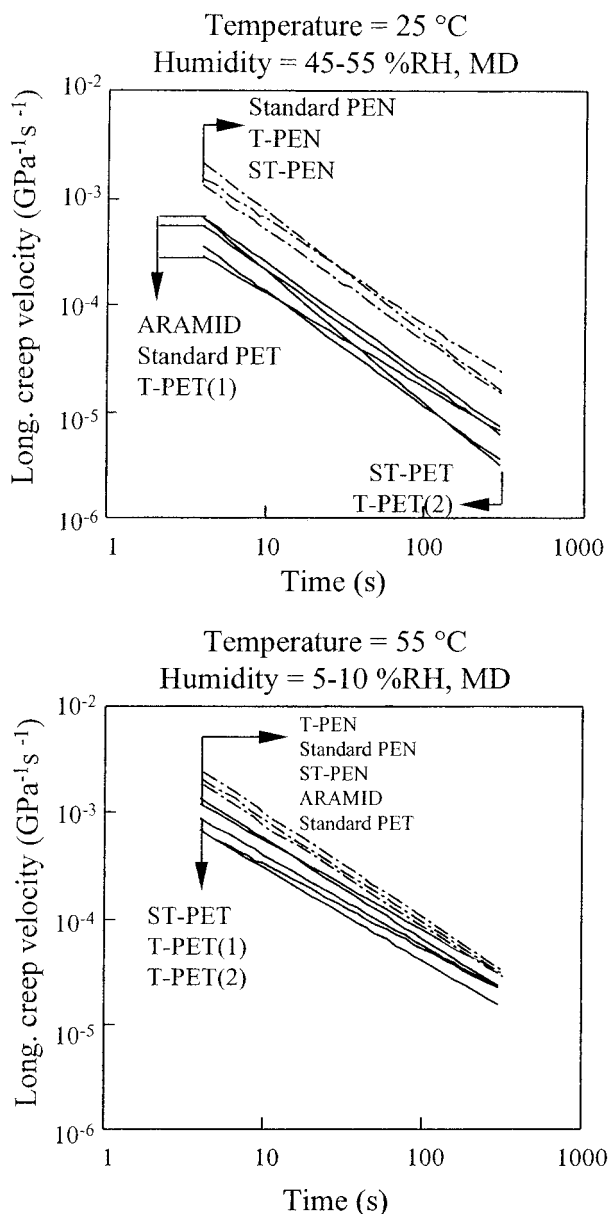


**Figure 11** Longitudinal short-term creep velocities for polymeric films at 25°C, 45–55% RH, and 55°C, 5–10% RH.

It is quite clear that PEN films show a higher residual creep compliance than that of PET films and ARAMID. At 25°C, the 2-s residual creep compliance of T-PEN is 0.021, 0.025, 0.031, and 0.052  $\text{GPa}^{-1}$  after 10, 30, 60, and 300 s creep, respectively, several times higher than that of T-PET(1), which is, correspondingly, 0.007, 0.017, 0.023, and 0.019  $\text{GPa}^{-1}$ . At 55°C, all the films show residual creep compliance not close to zero, even after a very short period of loading. Still, PEN films show a higher residual creep compliance than that of PET films, especially tensilized PET films.

According to viscoelastic theory, the deformation behavior of a polymer is determined by its loading history, and recovery can be regarded as a reversed creep processing. The residual creep compliance is not

affected by the elastic property of the material, but by the viscoelastic property. The material with low creep acceleration shows low residual creep compliance, and this corresponds to good mechanical stability for the magnetic tape substrate.

From the logarithm scale of creep curves in Figure 10 and creep velocity in Figure 11, it is clearly seen that the creep velocity for PET films is lower than that for PEN and ARAMID films. Thus, the creep elongations (not elastic deformation) of PET films are significantly lower than those of PEN films, and this corresponds to their low residual creep compliance as shown in Figure 9.

#### Long-term creep behavior

Creep compliance measurements for polymeric films are shown in Figure 12 for 25°C, 50–60% RH, 55°C; 5–10% RH; and 55°C, 80% RH.<sup>6</sup> The data sets are plotted on a linear scale and a log–log scale. Corresponding data are also summarized in Table V. ARAMID and tensilized PET films show a low increase of deformation at all the conditions, whereas PEN films show a larger increase. As per a comparison of creep compliance, ARAMID shows the lowest creep. The total amount of creep compliance is considerably smaller for tensilized-type PET than for PEN at all the temperature levels, and standard PET shows the largest amount of creep. It should be noted that more tensilization is likely to result in less creep for both PET and PEN, which is obvious for PET. Creep compliance measurements at 40°C, 15–25% RH, and 25°C, 50–60% RH, show similar trends<sup>6</sup> and are not presented in this article.

Temperature-dependent creep compliance at 100 h is summarized in Figure 13.<sup>6</sup> For ARAMID and tensilized-type PET, creep compliance is relatively constant, whereas the creep compliance for PEN and standard PET increases with an increase in temperature. This means that PEN and standard PET have more molecules with a higher mobility at a higher temperature in the current testing conditions.

The environmental condition, 55°C and 80% RH, is the upper limit of the operating envelop for the polymeric films used as a substrates for magnetic tapes. Water molecules are likely to enter into polymeric molecules and cause higher mobility to polymeric chains. In other words, the effect of a higher humidity condition is as much as is an increase in the temperature. Note that water molecules cannot enter into the crystalline region but can into an amorphous region in the polymer structure, since the amorphous region has a space where water molecules can be absorbed. Bhusan<sup>1</sup> suggested that, at higher humidity, water vapor plasticizes the film, which lowers the glass transition temperature and increases creep. The effect is likely to be seen both in PET and PEN. From Figure 12,

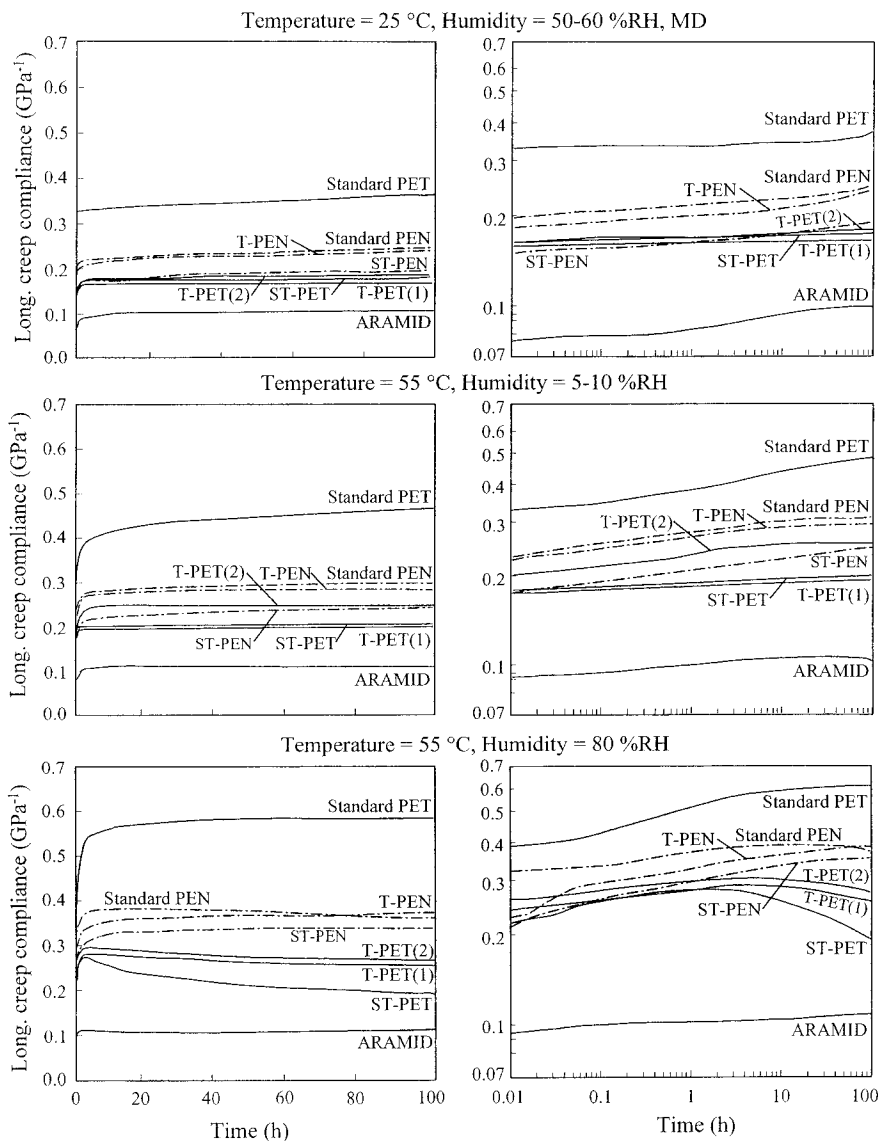


Figure 12 Creep compliance measurements for polymeric films at 25°C, 50–60 % RH; 55°C, 5–10% RH; and 55°C, 80% RH, plotted on linear scale and logarithm scale.

ARAMID shows less of an effect from high humidity. ARAMID contains amide groups, which have intermolecular hydrogen bonds. To take an example of

polyamide, nylon contains amide groups and the presence of moisture has a dramatic effect on the mechanical behavior.<sup>14</sup> This means that absorbed water molecules reduce the effect of interchain hydrogen bonds. For ARAMID, however, the creep property is unlikely to be influenced by water molecules. For this reason, it is highly probable that ARAMID consists of greatly rigid molecule substituents and leads to higher packing and lower space.

TABLE V  
Long-term Longitudinal Creep Compliance (GPa<sup>-1</sup>) of Polymeric Films at 7 MPa and Various Conditions

Sample	25°C, 50–60% RH			55°C, 5–10% RH		
	1 h	10 h	100 h	1 h	10 h	100 h
Standard PET	0.324	0.330	0.366	0.369	0.420	0.470
T-PET(1)	0.161	0.161	0.170	0.184	0.194	0.193
T-PET(2)	0.166	0.168	0.180	0.231	0.250	0.252
ST-PET	0.167	0.169	0.176	0.187	0.199	0.189
Standard PEN	0.211	0.220	0.246	0.267	0.290	0.296
T-PEN	0.196	0.210	0.239	0.264	0.282	0.285
ST-PEN	0.162	0.168	0.183	0.204	0.223	0.244
ARAMID	0.086	0.096	0.102	0.102	0.109	0.101

Some decrease of creep compliance was detected during the creep measurements of the tensilized-type PET with the 55°C/80% RH test. This means that tensilized-type PET shows competitive behavior between creep deformation and shrinkage during the long-term creep test. As discussed earlier, increased humidity can be regarded to have an effect similar to that of increased temperature as far as the effect on the

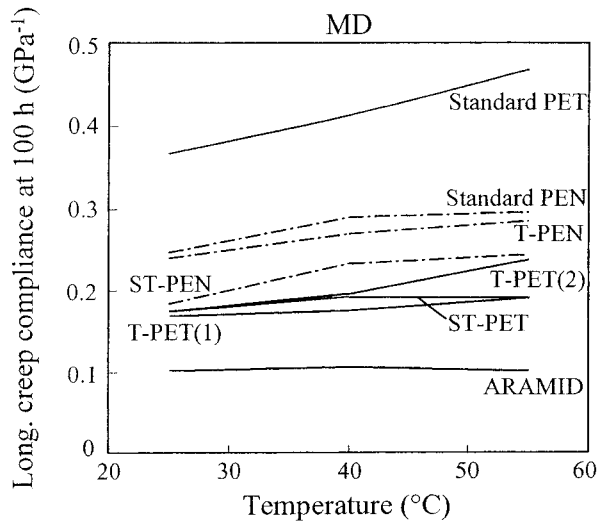


**Figure 13** Temperature dependency of the creep compliance at 7 MPa stress in the MD and 100 h.

molecular motion and relaxation of residual stress in the polymeric films is concerned. Recall the discussion in the section of short-term creep, that the creep velocities for PET and PEN films are closer at 55°C than they were at 25°C. It is not difficult to understand that PET films have a greater effect from humidity than do PEN films at 55°C, because the condition of 55°C and 80% RH might have a similar effect of an increase in temperature close to the glass transition temperature of PET. From the fact that all the tensilized PET films show decreased creep compliance at the 55°C, 80% RH test, we draw the conclusion that tensilized PET films contains more residual stresses than do standard PET and can be relaxed at critical application conditions and results in more dimension deflection–shrinkage. PEN films were less affected by the high humidity at 55°C, because they have a higher glass transition temperature than that of PET films.

*Prediction of long-term creep behavior using time–temperature/humidity superposition.* Based on the data of creep compliance, master curves were generated to predict long-term creep behavior at ambient temperature after several years, using a time–temperature superposition technique to estimate the creep deformation of the substrates during storage at ambient temperature for long periods.<sup>1</sup> This analytical method is applied on the ground that most polymer materials will behave in the same manner at a particular high temperature, as they will when they are deformed on a long time scale at a lower temperature. Results from this analysis are presented in Figure 14 for the MD to predict the creep compliance at 25°C as the reference temperature over 10<sup>6</sup> h (approximately 100 years).<sup>6</sup> Creep experiments at a temperature higher than the 25°C reference temperature correspond to a longer time period. Therefore, the curves of 40 and 55°C were shifted to the

right. The shift factors show how much each curve was shifted to enable a smooth curve to be obtained. Some vertical shifting is also necessary to accommodate differences in the initial elastic response when the film samples are loaded as well as differences in the elastic moduli at elevated temperature. However, this vertical shifting rarely exceeds 5% of the total creep compliance measured for a polymer.

According to the master curves shown in Figure 14, ARAMID shows the lowest amounts of creep. It is clear that tensilized-type PET also shows considerably lower creep deformation. In contrast, PEN shows somewhat more creep at all time periods, and standard PET has the largest amounts of creep. The slopes of the curves in Figure 14 indicate the creep velocity. It

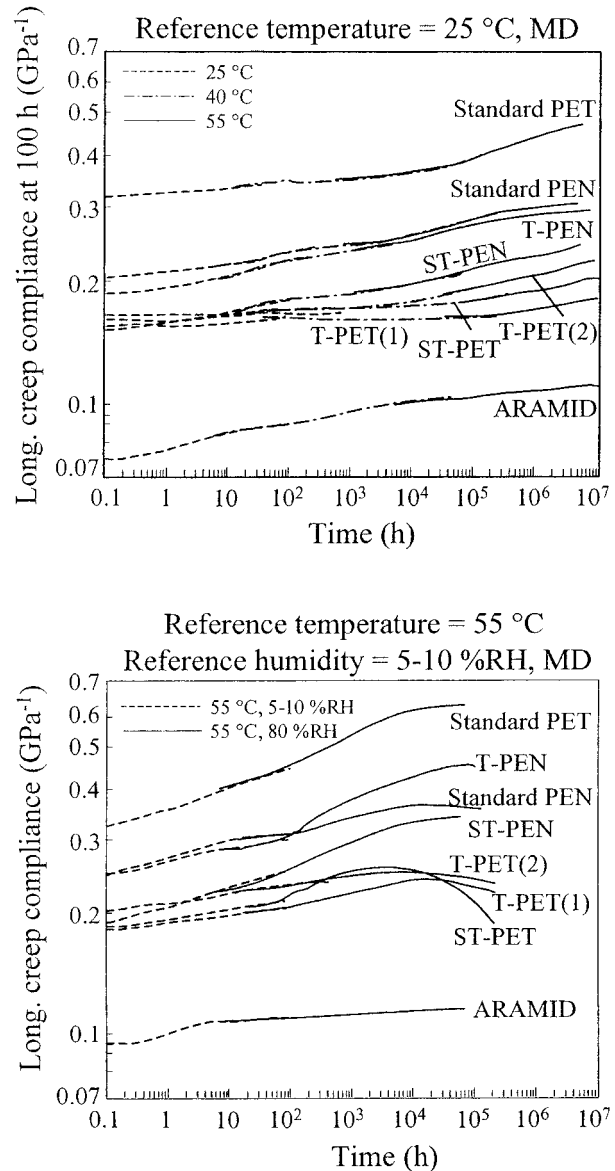


**Figure 14** Creep compliance master curves at (a) 25°C reference temperature and (b) 55°C reference temperature and 5–10% RH reference humidity for polymeric films.

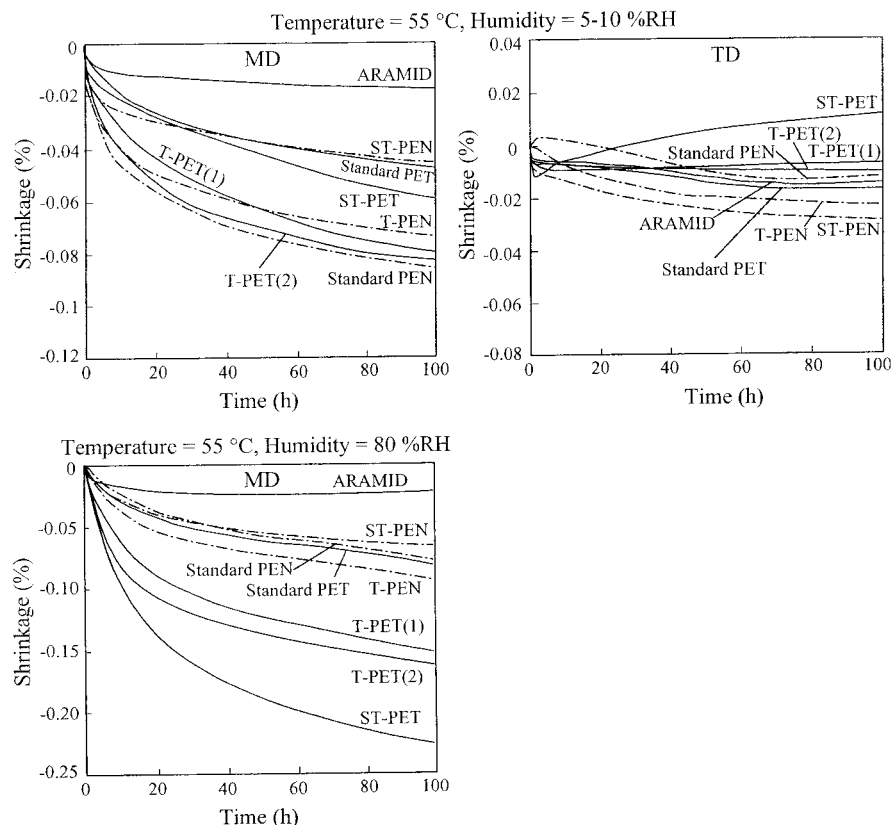


**Figure 15** Shrinkage measurements for polymeric films at 55°C, 5–10% RH in the MD and the TD and 55°C, 80% RH in the MD.

is also useful to consider the overall slope of the master curve from 0.1 to  $10^6$  h: Tensitized-type PET has the lowest velocity of creep and ARAMID has a similar creep velocity to that of PEN, and this is consistent with the result in the short-term creep section. However, the creep velocity of ARAMID turns out to be low at a longer time, while PEN and standard PET have creep velocity that increases throughout the experiments.

Master curves were also generated to predict long-term creep behavior at a 5–10% RH level. The analytical technique is known as time–humidity superposition,<sup>1</sup> similar to time–temperature superposition. Using this technique, creep measurements at elevated humidity at the same temperature were superimposed to predict the behavior at low humidity and longer time periods. The methodology is based on the same grounds as is the time–temperature superposition. The results of this above analysis are presented in Figure 14 for the various films in the MD to predict the creep compliance at 55°C and 5–10% RH as the reference temperature and humidity over  $10^5$  h (about 11 years). The lowest amount of creep is shown for ARAMID, followed by tensitized-type PET, PEN, and standard PET. This prediction is similar to the time–temperature superposition master curve, except that

the tensitized PET films show obvious shrinkage at a long period.

*Shrinkage measurements.* Shrinkage data are presented in Figure 15 in both the MD and the TD at 55°C, 5–10% RH,<sup>6</sup> and in the MD at 55°C, 80% RH. The shrinkage behavior can be directly related to the polymeric structure and processing history. Shrinkage is a nonrecoverable deformation that can be attributed to the relaxation of oriented molecules in the amorphous regions of the films.<sup>1,24–28</sup> In other words, shrinkage arises from the disorientation (relaxation) of the oriented amorphous phase into a more random state and results in the removal of the residual stresses formed during processing of the films. Note that the oriented molecules in the amorphous region can be distinguished from the highly oriented molecules in the crystalline regions of the polymers. As a result, a total contraction of the films could occur in the orientation direction, and, in this study, shrinkage was found to be larger in the MD along with the more oriented direction.

All the films shrank at 55°C in the MD; also, all the eight films shrank more at 80% RH than that at 5–10% RH. ARAMID shows the lowest shrinkage at the both humidity conditions. At 55°C, 5–10% RH, the shrinkage of standard PEN, T-PEN, and ST-PEN are 0.08,

0.07, and 0.04%, respectively. More tensilization appears to result in lower shrinkage for tensilized-type PEN at 55°C, 5–10% RH. This can be accounted for by the fact that all the materials were in a glassy state during the test. More tensilization increases oriented elements and makes the elements more resistance to shrinkage. Shrinkage for standard PET is small due to a low draw ratio in this direction.

At 55°C, 80% RH, ST-PEN still shows lower shrinkage than that of standard PEN and T-PEN, which indicates that an oriented PEN molecular structure has good shrinkage resistance at this condition, and the films' behavior is typical of the glassy state. But for PET films, it is quite clear that more tensilization results in more shrinkage. Also, all the tensilized PET films show, obviously, higher shrinkage than that of the PEN films.

As the mobility of molecular segments is of concern, an increase of humidity can be effectively equivalent to an increase of the temperature.<sup>21</sup> Thus, 55°C, 80% RH, may be equal to a condition of low humidity but higher temperature, which is close to the glass transition temperature of PET films (about 80°C). In such a case, the large-scale movement of the molecular backbone encourages the relaxation of the residual strain and/or stress and results in significant shrinkage. The amount of shrinkage, or the driving force, is determined by the level of residual strain, which is high in tensilized films. That is why ST-PET shows more shrinkage than do T-PET(2) and T-PET(1), and they all shrink more than does standard PET. This is further confirmed by ref. 6: The shrinkage data for standard PET, T-PET(1), and ST-PET in the MD at 10°C, 30 min, were reported as 0.7, 1.2, and 2.4%, respectively. Compared to PET films, the glass transition temperature of PEN films is about 120°C, which is significantly higher than is the effective temperature of 55°C, 80% RH. So, PEN films behave as in a typical glassy state and show less shrinkage than do PET films at this condition.

### Poisson's ratio, lateral creep, and CHE

#### Poisson's ratio

The Poisson's ratio data for various polymeric films at different temperatures and humidities are summarized in Table VI. The values for these polymeric films are between 0.29 and 0.53 at the test conditions. PEN films, in general, have higher Poisson's ratio values than those of PET films, and ARAMID has a high, but constant, value between 0.44 and 0.47 at various conditions.

It was discussed in previous sections that tensilization processing can significantly reduce the elastic and viscoelastic deformations of the polymeric films in the MD. But this beneficial effect is attenuated for the lateral deformation behavior, since the data in Table

**TABLE VI**  
Poisson's Ratio of the Magnetic Tape Substrates at Various Conditions (Deviation is Within 5%)

Sample	25°C, 15% RH	25°C, 50% RH	25°C, 80% RH	40°C, 50% RH
Standard PET	0.29	0.30	0.32	0.30
T-PET(1)	0.32	0.33	0.33	0.34
T-PET(2)	0.32	0.33	0.33	0.34
ST-PET	0.36	0.39	0.37	0.53
Standard PEN	0.32	0.35	0.37	0.33
T-PEN	0.38	0.38	0.38	0.41
ST-PEN	0.44	0.43	0.42	0.47
ARAMID	0.44	0.44	0.47	0.44

VI show that the Poisson's ratios for tensilized films are higher than those for standard films, for both PET and PEN films. For example, at 25°C, 50% RH, the Poisson's ratio for standard PET, T-PET(1), and ST-PET are 0.30, 0.33, and 0.39, respectively, and the value for standard PEN, T-PEN, and ST-PEN are 0.35, 0.38, and 0.43, respectively. The reason for this is not fully clear, since no systematic study on the Poisson's ratio for polymeric films has been reported. We conjecture that this may be due to the weakening effect of the tensilization on the mechanical stiffness of polymeric films in the TD. The Poisson's ratio of polymers is determined by the deformation characteristics of molecular chains or groups, which is modified by the manufacturing processing. Tensilization stretches or rotates some molecular segments so that they align in the tensilization direction; this increases the fraction of unidirectionally aligned chains and makes them more difficult to deform further in the tensilization direction: the MD. At the same time, the stiffness and the interlinking of molecules in the TD is weakened. This is evidenced by the fact that tensilized films have a significantly lower Young's modulus in the TD than that of balanced films (Table II). As a result, when the films are stressed in the MD, more contraction in the TD is observed.

What should be kept in mind is that, although the Poisson's ratios for tensilized films are high, it does not necessarily mean that they are more liable to deform in the lateral direction than are standard films. The data in the following section of lateral creep will show that tensilized films have a lower lateral creep deformation as compared to those of the standard films, when the same longitudinal stress (7 MPa) is applied. This is because the tensilized films have significantly higher moduli and lower elongation in the longitudinal direction compared to the standard films.

In comparing the data at 25°C, 50% RH, and 40°C, 50% RH, increased temperature results in an increase of the Poisson's ratio, and this is more significant for tensilized films than for standard films. When the temperature increases from 25 to 40°C, the Poisson's ratio values for standard PET, T-PET(1), and ST-PET

changes from 0.30, 0.33, and 0.39 to 0.30, 0.34, and 0.53, respectively (as summarized later in Fig. 19). The higher the tensilization ratio, the greater is the increase in the Poisson's ratio. It is believed that the mechanism of the effect of temperature on the Poisson's ratio is molecular orientation-related. Since for standard films the stretch ratios along the MD and the TD (during the manufacturing) are similar, their molecular chain orientation are balanced in the MD and the TD and their Poisson's ratios are less affected by the change of temperature.

It has been known that effects of humidity on the polymer are similar to that of temperature in some aspects, such as that both the hygroscopic and thermal expansions are reversible; an increase of both of them may increase the polymer's deformability and stress relaxation, etc. From Table VI, it can be seen that an increase of humidity generally increases the Poisson's ratio. But tensilization reduces or even reverses this tendency. For example, at 25°C, 15, 50, and 80% RH, the Poisson's ratio values for standard PEN are 0.32, 0.35, and 0.38, respectively, the values for T-PEN are constant at 0.38, and the values for ST-PEN are 0.44, 0.43, and 0.42, respectively. Possibly, this can be explained as follows: After tensilization, a large fraction of molecular chains are oriented in the MD, so the interstitial positions that water molecules reside at are mostly along the TD direction, among the oriented molecular segments. Or, in other words, the water absorption will result in more swelling in the TD than in the MD, and the CHE in the TD is higher than in the MD for the films tensilized in the MD (this will be discussed in the following section). Thus, the effect of water molecules on the mechanical properties of tensilized films in the TD is larger than that in the MD. The interstitial water molecules not only result in hygroscopic expansion in the TD, but also hold the space between the oriented molecules and prevent them from contraction when the film is loaded in the MD. Also, the hydrogen bonds formed by water molecules and polymer groups reduce the residual stresses in these areas, and the system's potential energy is lowered. As a result, the lateral contraction is restrained due to the water absorption while the longitudinal elongation is encouraged due to the release of residual stresses, so the Poisson's ratio is reduced.

As for standard films, because the Young's modulus of standard films in the TD is slightly higher than that in the MD, there are probably more molecular segments oriented in the TD than in the MD. So, the Poisson's ratios of balanced films increase slightly when relative humidity increases in a large range. Note that the water molecule enters only into the amorphous region of polymeric films, and PET films have a higher crystallinity than that of PEN films, so the effect of humidity is more obvious for PEN films than for PET films.

### Lateral creep

Figure 16 shows long-term lateral creep data for various polymeric films and the effect of temperature (from 25 to 40°C) and humidity (from 15 to 80% RH), when the films are loaded at a 7 MPa stress along the MD. The lateral creep deformation data at 30 s and 50 h are also tabulated in Table VII. All the samples show a continuous increase in lateral creep during the tests at all the conditions. ARAMID shows the lowest lateral creep deformation among the samples, while standard PET shows the highest. In general, PEN films show higher lateral creep deformation than do tensilized PET films. It is obvious that tensilized films have a lower lateral creep deformation than that of standard films, which is consistent with the results of the longitudinal creep tests.

As the temperature increases, the lateral creep deformation for all the samples increase, but for PET films, it increases more. The effect of temperature on the long-term dimensional stability of polymeric films depends mainly on the glass transition temperature. The polymer with a high glass transition temperature usually shows good dimensional stability, due to its high molecular structural stiffness. The glass transition temperature for PEN is about 40°C higher than that for PET. This ensures that PEN films are less affected by the increase of temperature than are PET films. For the reasons discussed earlier, the effect of humidity on PEN films is more significant than that on PET films, as shown in Figure 16.

### CHE

The CHE data for various polymeric films in the MD and the TD at 25°C, 20–80% RH, are listed in Table VIII. PET and PEN films have similar CHE values in the current tests, and ARAMID has a relatively low CHE in both the MD and the TD. Tensilized films show a lower CHE than that of standard films in the MD. For example, the CHE data for standard PET, T-PET(1), and ST-PET in the MD are 10.3, 5.9, and 5.0  $\times 10^{-6}/\%$  RH, respectively. Now, we can verify the assumption in a previous section that the interstitial positions for a water molecule are mainly along the TD direction for tensilized films. From the data in Table VIII, the CHEs for all the tensilized films are higher in the TD than in the MD.

### Thermal expansion data

Table VIII summarizes the CTE data of polymeric films in the MD and the TD at various temperature ranges. The data are also plotted in Figure 17. As temperature increases, the CTE for most samples increases and covers a large range from  $-12$  to  $26 \times 10^{-6}/^{\circ}\text{C}$ . The tensilized films have a lower CTE in

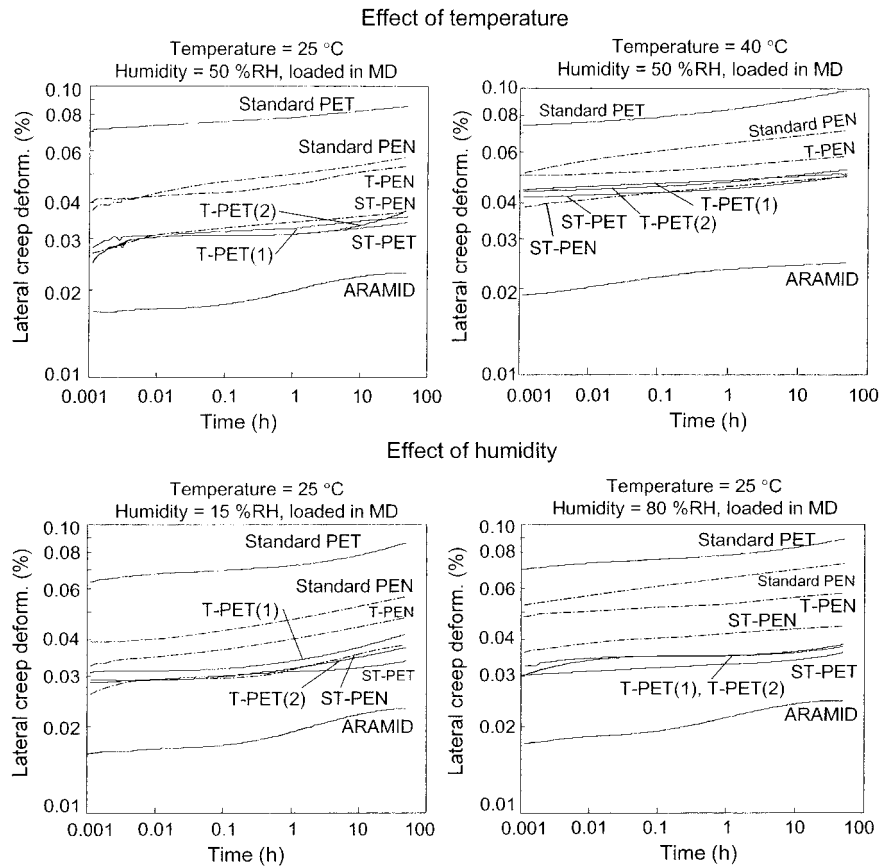


**Figure 16** Long-term lateral creep for the polymeric films at various environmental conditions, showing the effect of temperature (25–40°C, 50% RH) and humidity (25°C, 15–80% RH).

the MD and a higher CTE in the TD than those of standard films, and this is true for both PET and PEN films. High tensilization results in more oriented molecules and residual shrinking stress in this direction; both factors make it more difficult to thermally expand in the corresponding direction. At 60–70°C, the CTE for T-PET(2) and ST-PET in the MD begins to decrease, while data for all the other samples still increase. We believe this is due to the relaxation of residual stress in these two films. Tensilization can be used as a method to control the CTE.

The CTE data for some samples in the thickness direction, measured by Osawa,<sup>16</sup> are listed in Table IX. The values are on the order of  $200 \times 10^{-6}/^{\circ}\text{C}$ , one or two decades higher than the in-plane CTE data. The reason lies in the fact that molecules of polymeric films are aligned in planar directions, either in the MD or the TD. The mechanical stiffness and dimensional stability of polymeric films in a nonoriented direction is significantly lower than that in an oriented direction(s), since the molecules are arranged in a loose manner in this direction. The CTE in the thickness

**TABLE VII**  
Lateral Creep Deformation (%) of Magnetic Tape Substrates at a Stress of 7 MPa in MD

Sample	25°C, 50% RH		40°C, 50% RH		25°C, 15°C		25°C, 80% RH	
	30 s	50 h	30 s	50 h	30 s	50 h	30 s	50 h
Standard PET	0.073	0.085	0.076	0.099	0.067	0.086	0.073	0.089
T-PET(1)	0.030	0.037	0.046	0.051	0.031	0.042	0.034	0.038
T-PET(2)	0.031	0.036	0.045	0.052	0.029	0.038	0.034	0.038
ST-PET	0.030	0.034	0.043	0.050	0.029	0.034	0.031	0.036
Standard PEN	0.043	0.057	0.056	0.072	0.040	0.056	0.056	0.073
T-PEN	0.042	0.053	0.050	0.058	0.035	0.048	0.050	0.058
ST-PEN	0.031	0.037	0.041	0.049	0.029	0.038	0.039	0.045
ARAMID	0.018	0.025	0.020	0.025	0.017	0.023	0.018	0.025

**TABLE VIII**  
CTE ( $10^{-6}/^{\circ}\text{C}$ ) and CHE ( $10^{-6}/\% \text{RH}$ ) of Magnetic Tape Substrates

Sample	CTE in MD and TD directions								CHE	
	30–40°C		40–50°C		50–60°C		60–70°C		25°C, 20–80%RH	
	MD	TD	MD	TD	MD	TD	MD	TD	MD	TD
Standard PET	8.5	-5.2	16.3	2.4	20.9	5.0	23.8	8.5	10.3	7.8
T-PET(1)	-5.2	6.4	-0.4	15.5	1.0	20.6	1.5	26.5	5.9	11.7
T-PET(2)	-4.5	1.9	-0.4	14.2	1.9	20.9	2.0	25.7	6.1	11.0
ST-PET	-6.2	-3.5	1.6	17.1	3.6	22.9	-2.3	20.7	5.0	8.4
Standard PEN	5.2	-9.2	3.2	-1.7	8.8	3.0	11.0	5.3	8.2	8.7
T-PEN	-6.3	2.5	0.9	7.8	5.8	11.5	8.3	14.6	7.9	10.6
ST-PEN	-11.9	6.5	-5.2	12.7	-0.4	17.1	3.4	20.1	5.8	12.6
ARAMID	-3.3	-2.1	-2.8	3.2	9.7	9.5	14.0	3.6	-2.7	9.2

direction is much higher than that in the TD and the MD, which is consistent with trend for the CTE for tensilized films in planar directions as the CTE is higher in the TD than in the MD. Also, as we reported in the previous section, the Poisson’s ratio values for tensilized films are higher than those for standard films.

Figure 18 shows the effect of tensilization on the physical and mechanical properties of polymeric films. For both PET and PEN films, as the tensilization ratio increases (storage modulus increases), the CTE decreases in the MD and increases in the TD (note that tensilized films have lower moduli than those of standard films in the TD). The same tendency occurs for CHE. These are believed to be contributed by the oriented elements in tensilized films.

**Summary of selected data**

To gain a perspective, the physical and mechanical properties of ultrathin polymeric films are tabulated in Table X. Figure 19 also shows the deformability of polymeric films at various conditions, which include elastic deformation in the MD and the TD at 7 MPa stress; longitudinal creep deformation at 55°C, 100 h;

lateral creep deformation at 40°C, 50 h; shrinkage at 55°C, 100 h, in the MD and the TD; and thermal expansion from 30 to 55°C and hygroscopic expansion from 25 to 75% RH.

**Degradation of substrates after tape manufacturing**

Figure 20 shows a comparison of the storage modulus and lateral creep deformation for some tape substrates (with front and back coats removed) and corresponding never-coated virgin films.<sup>11,12</sup> For the storage modulus in the MD, all four substrates show strengthening after tape manufacturing, with the PEN substrate for the ME tape showing the most significant improvement. For the lateral creep deformation, PET films show degradation and PEN films show enhancement. The reason is believed to be due to two counteracting aspects: thermal relaxation on the oriented structure and thermal setting on the amorphous regions. PEN films have a higher glass transition temperature than that of PET films, which makes them dimensionally stable during the tape-manufacturing processing at high temperatures.

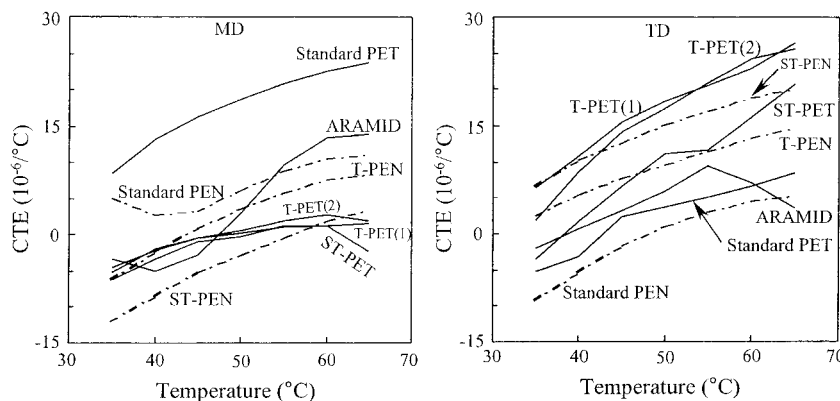


**Figure 17** Coefficient of thermal expansion as a function of temperature for various polymeric films in the MD and the TD.



TABLE IX  
CTE ( $10^{-6}/^{\circ}\text{C}$ ) In-Plane and Thickness Direction<sup>16</sup>

Sample	In-plane (40–50°C)		Thickness direction
	MD	TD	
T-PET(2)	-3.0	19.0	192
T-PEN	1.3	8.7	194
ST-PEN	-2.3	12.9	198

### Relationship between the mechanical, hygroscopic, and thermal properties and molecular structure of polymeric films

The mechanical properties of polymeric films are dependent on their molecular configuration and conformation. PEN contains a naphthalene ring that is more rigid than is the benzene ring for PET. This is why the PEN films have higher moduli, strength, and glass transition temperatures than those of PET films. Also, PEN films show more thermal stability than that of PET films, which is desirable in tape manufacturing and storage at high temperature and high humidity (such as 55°C, 80% RH).

There is no oxygen atom in the ARAMID backbone chain; instead, it consists of an aromatic hydrocarbon group (benzene ring) combined by amide bonds, *para*-

linked by intermolecular hydrogen bonds among amide groups, and interlinks among substituent chains, which are stronger than are the intermolecular interactions for PET and PEN. Also, the molecular configuration for ARAMID is highly symmetric. As a result, ARAMID enables the formation of high-strength, high-modulus, and low strain-at-yield and strain-at-break polymer film.

Crystallinity plays an important role in determining the mechanical properties of polymeric films. The secondary relaxation, which controls the viscoelastic properties of polymeric films at ambient temperature, occurs extensively in the amorphous regions, which have higher mobility than that of the crystalline regions. Cakmak and Wang<sup>29</sup> suggested that the increase in crystallinity and orientation of chains in the amorphous region results in a reduction in creep strains for PET. Mascia and Fekkai<sup>30</sup> indicated that when the degree of crystallinity of PET reached 43% the shrinkage would be completely suppressed. The network structure formed by the crystalline region significantly improves the stiffness and mechanical stability by anchoring polymeric chains in the high-density and less mobile crystalline region. The crystallinity of PET films is higher than that of PEN films,

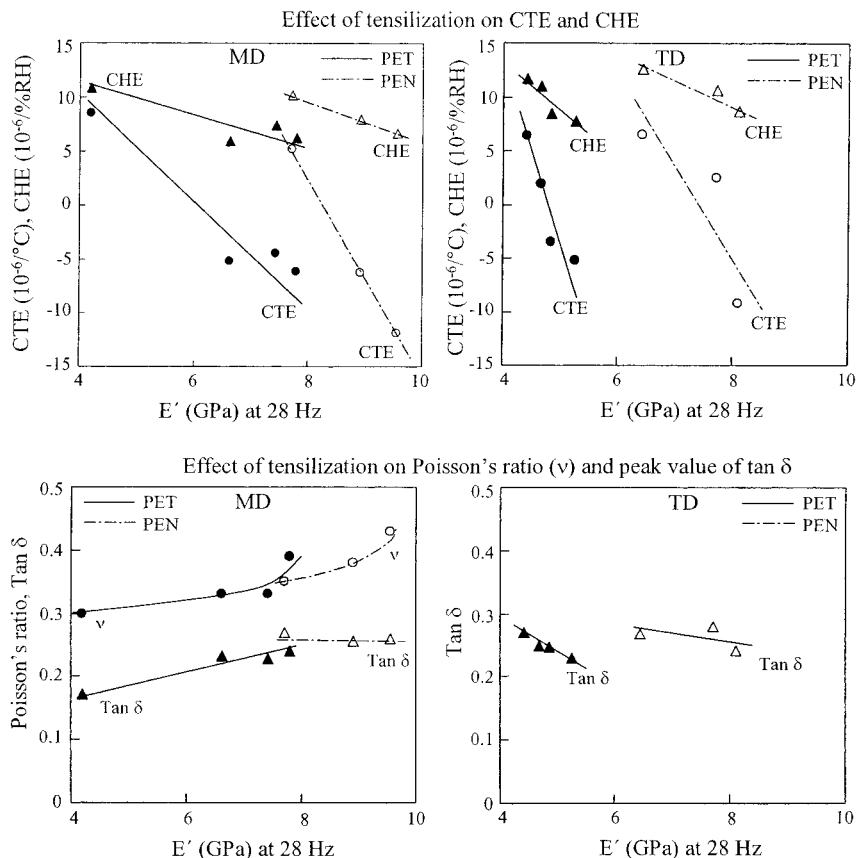


Figure 18 Relationship between the storage modulus and physical and mechanical properties of polymeric films: effect of tensilization on CTE, CHE, Poisson's ratio and peak value of the loss tangent.

TABLE X  
Summary of Mechanical, Thermal, Hygroscopic, and Dimensional Stability Characteristics  
of Magnetic Tape Substrates

Sample		Density <sup>a</sup> (g/cm <sup>3</sup> )	$T_g^{b,c}$ DSC <sup>b</sup> / DMA <sup>c,d</sup> (°C)	CTE <sup>e</sup> (30–40°C) (10 <sup>-6</sup> / °C)	CHE <sup>e</sup> (25°C) (15–85%) (10 <sup>-6</sup> / RH)	$T_m^a$	Poisson's ratio <sup>e</sup> (25°C, 50% RH)	Tensile properties <sup>d,f</sup> (22°C, 50% RH)				
								$E$ (GPa)	F5 (MPa)	$\epsilon_y$ (%)	$\sigma_b$ (MPa)	$\epsilon_b$ (%)
Standard	MAJ	1.395	80/110	8.5	10.3	263	0.30	3.30	95	3.00	200	115
PET	MIN			-5.2	7.8			4.54	117	4.10	266	79
T-PET(1)	MD		/110	-5.2	5.9		0.33	6.30	172	3.10	350	44
	TD			6.4	11.7			4.10	106	2.80	230	108
T-PET(2)	MD		/105	-4.5	6.1		0.33	7.45	166	3.20	414	51
	TD			1.9	11.0			4.90	109	2.00		
ST-PET	MD		/110	-6.2	5.0		0.39	7.15	195	3.30	461	45
	TD			-3.5	8.4			4.47	107	3.20	257	75
Standard	MD	1.355	120/150	5.2	8.2	272	0.35	6.25	175	3.20	334	42
PEN	TD			-9.2	8.7			6.90	200	3.20	384	42
T-PEN	MD		/150	-6.3	7.9		0.38	6.50	190	2.60	340	30
	TD			2.5	10.6			5.60	158	2.90	300	40
ST-PEN	MD		/150	-11.9	5.8		0.43	7.80	220	2.70	452	36
	TD			6.5	12.6			5.42	144	2.65	293	75
ARAMID	MD	1.500	280/—	-3.3	-2.7	None	0.44	20.4	628	2.80	638	6.4
	TD			-2.1	9.2			11.3	338	3.80	433	11

$T_g$ , glass transition temperature;  $T_m$ , melting point;  $E$ , modulus of elasticity; F5, stress at 5% strain;  $\epsilon_y$ , strain at yield;  $\sigma_b$ , breaking strength;  $\epsilon_b$ , strain at break.

<sup>a</sup> Ref. 1.

<sup>b</sup> Ref. 6.

<sup>c</sup> Determined from the peak of the loss tangent using DMA with the frequency at 0.016 Hz.

<sup>d</sup> Ref. 7.

<sup>e</sup> This work.

<sup>f</sup>  $E$  taken at 0.1/min strain rate. Other properties: data for PET and PEN films taken at 0.5/min strain rate; data for ARAMID taken at 0.1/min strain rate.

as schematically shown in Figure 21,<sup>6</sup> due to the inhibition of the large naphthalene ring in the molecular movement during the crystallization. That is why the mechanical properties of PET films are less affected by the factors that mainly affect the amorphous region, such as deformation, frequency, long time duration, and humidity.

An orientation structure resulting from tensilization can significantly increase the modulus and dimensional stability and reduce the CTE and the CHE in its direction (e.g., the MD), but has a reversed effect on the properties in the other direction (say, the TD). This can also be seen from the Poisson's ratio for tensilized films, which are higher than that for standard films. Residual stress stored in the oriented structure is released at the glass transition temperature and results in a high peak value of the loss tangent.

## CONCLUSIONS

Tensile and DMA tests showed that ARAMID has the highest modulus and breaking strength among the polymeric films. The MD-tensilized films have

higher moduli and strength, but lower strain at yield and strain at break than those of the standard films along the MD. This relationship is reversed in the TD. PEN films have a higher frequency dependence as compared to PET films. PEN films exhibit a higher elastic modulus at high frequencies than that of tensilized PET films comparable in degree. PET films have a lower rate of decrease in the storage modulus than that of PEN films as the temperature increases before their glass transition temperatures are reached. The loss tangent peak temperatures for PET and PEN films were determined as 110 and 140°C (at 0.016 Hz), respectively, and were not affected by tensilization. A high glass transition temperature is desired for tape manufacturing. The storage modulus and lateral creep resistance for PEN films were found to be enhanced after ME tape processing. According to the frequency-temperature master curve that covers a frequency range from 10<sup>-18</sup> to 10<sup>10</sup> Hz, the storage moduli for PET films were lower at high frequencies and higher at low frequencies (10<sup>-2</sup> Hz in the MD and 10<sup>-5</sup> Hz in the TD), compared to those of PEN films.

**TABLE X**  
Continued

DMA properties $E'$ at 50°C <sup>d</sup>		Longitudinal creep compliance			Lateral contraction <sup>e</sup> (7 MPa in MD, 50 h) 25–50/25–80/40–50 (%)	Shrink <sup>b</sup> (55°C, 5–10% RH, 100 h) (%)
		Short-term <sup>e</sup> (7 MPa, 30 s, 55°C, 5–10% RH) (GPa <sup>-1</sup> )	Long-term <sup>b</sup> (7 MPa, 100 h)			
(0.016 Hz) (GPa)	28 Hz (GPa)		(25°C, 50% RH)	55°C, 5–10%/80% RH)(GPa <sup>-1</sup> )	°C–% RH	
3.84	4.05	0.316	0.366	0.470/0.606		0.049
4.67	5.04				0.085/0.089/0.099	0.014
5.92	6.45	0.168	0.170	0.193/0.261		0.079
3.91	4.20				0.037/0.038/0.051	0.007
6.54	7.16	0.163	0.191	0.252/0.278		0.084
4.16	4.51				0.036/0.038/0.052	0.041
6.91	7.38	0.157	0.176	0.189/0.191		0.061
4.43	4.61				0.034/0.036/0.050	0.014
4.93	6.85	0.231	0.246	0.296/0.367		0.088
5.18	7.16				0.057/0.073/0.072	0.011
5.37	7.85	0.215	0.239	0.285/0.376		0.073
4.93	6.85				0.053/0.058/0.058	0.022
6.08	8.47	0.166	0.183	0.244/0.344		0.046
3.96	5.73				0.037/0.045/0.049	0.027
15.4	19.9	0.073	0.102	0.101/0.111		0.027
10.7	14.8				0.025/0.025/0.025	0.014

DMA: dynamic mechanical analysis; CTE: coefficient of thermal expansion; CHE: coefficient of thermal expansion

PEN films were found to have better damping properties than those PET films, which implies that they may have better performance in handling during the tape manufacturing. For short-term and long-term creep and shrinkage tests, ARAMID film showed the lowest creep compliance and shrinkage among all the samples. PEN films showed larger

creep compliance and creep velocity than those of PET films at the same test condition. However, in the creep test at 55°C, 80% RH, tensilized PET films showed obvious shrinkage, whereas PEN and ARAMID films did not. This is believed to be because the high humidity may have had an effect similar to an increase in the temperature, which

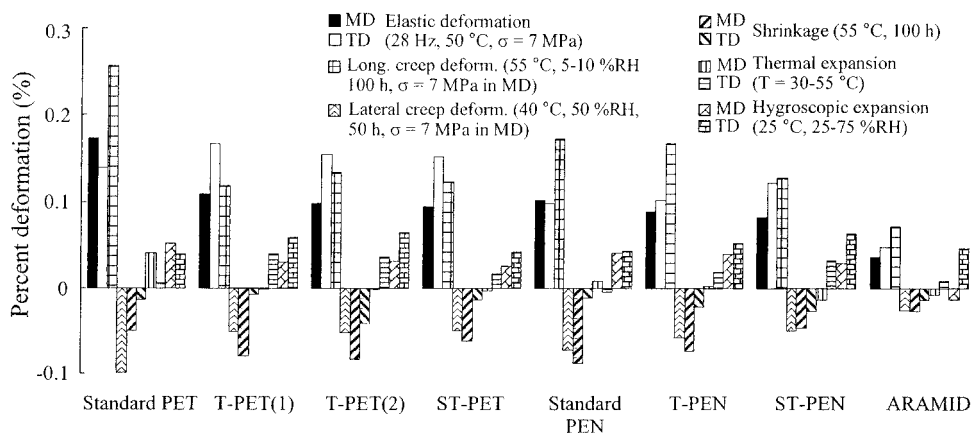


**Figure 19** Bar-chart summary of elastic, viscoelastic, and hygroscopic and thermal deformation for various polymeric films.

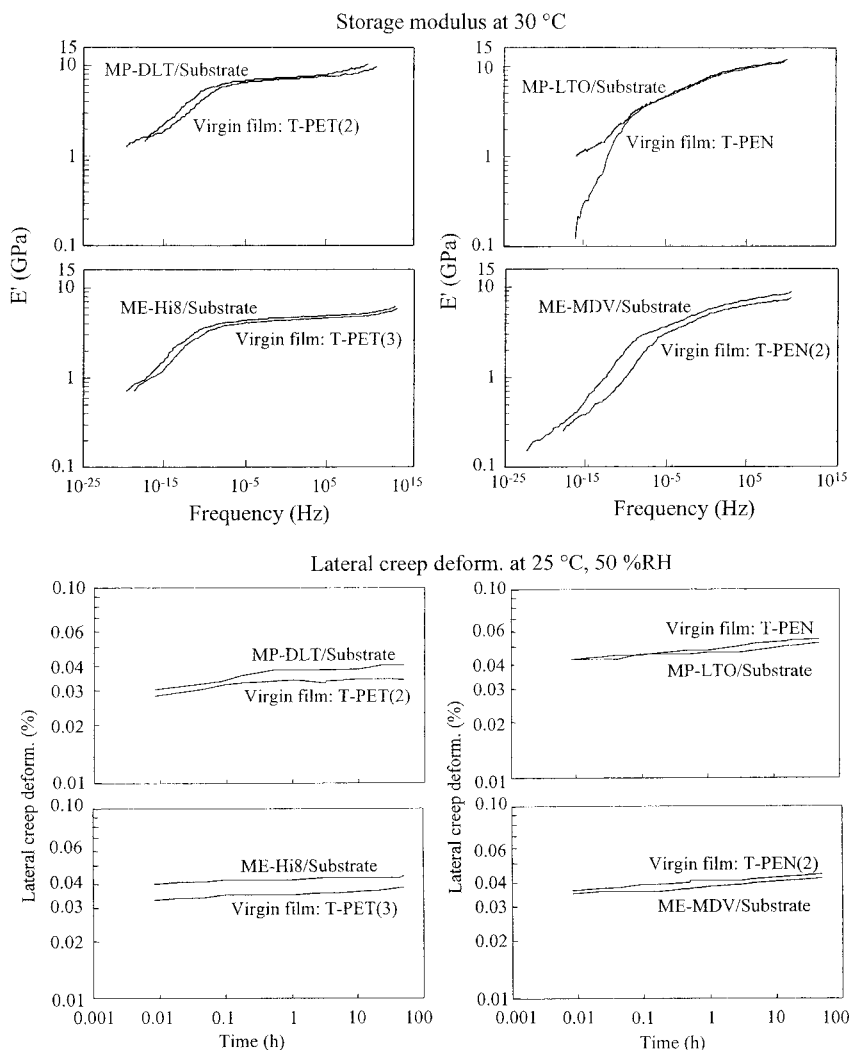


**Figure 20** Storage modulus and lateral creep deformation of tape substrate and virgin films, showing the degradation of substrates after MP and ME tape manufacturing.<sup>11,12</sup>

made the effective temperature close to the glass transition temperature for PET films.

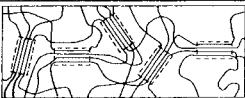
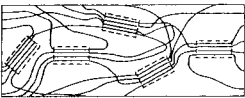
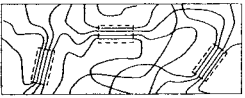
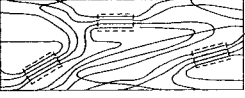
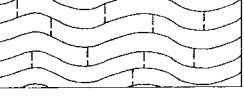
The Poisson's ratio values for polymeric films were found to be from 0.29 to 0.53. The tensilized films have a higher Poisson's ratio than that of standard films. The effects of temperature and humidity on the Poisson's ratio are related to the materials' molecular structure. Increased temperature has an obvious increase on the Poisson's ratio for PET films due to the fact that PET films have a relatively low glass transition temperature, while increased humidity has an obvious increase in the Poisson's ratio for PEN films because PEN films have lower crystallinity.

ARAMID film showed the lowest lateral creep deformation among the samples, followed by tensilized PET films and then PEN films. Tensilized films have a lower lateral creep deformation than that of standard films. Elevated temperature and humidity encourage the lateral creep for all the samples, but PET films are

more affected by the temperature and PEN films are more affected by the humidity.

PET and PEN films showed similar CHE values, while ARAMID had a relative low CHE in both the MD and the TD. As temperature increases, CTE values for all the samples increased in both the MD and the TD and covered a large range from  $-12$  to  $26 \times 10^{-6}/^{\circ}\text{C}$ . The tensilized films had a lower CTE in the MD and a higher CTE in DT than those in standard films, and this was true for both PET and PEN films. The CTE data along the thickness direction were reported in the literature to be one or two decades higher than the in-plane CTE data.

The research reported in this paper was supported by the industrial membership of the Nanotribology Laboratory for Information Storage and MEMS/NEMS (NLIM) at The Ohio State University. The authors would like to thank Mr. T. Higashioji of Toray, Japan, Mr. T. Osawa of DuPont-Teijin, USA, and Mr. H. Murooka of Teijin-DuPont,

Substrate	Structure	Comments
Standard PET		<ul style="list-style-type: none"> <li>•Low <math>T_g</math></li> <li>•Few oriented chains</li> <li>•High crystallinity</li> </ul>
Tensitized PET		<ul style="list-style-type: none"> <li>•Low <math>T_g</math></li> <li>•Many oriented chains</li> <li>•High crystallinity</li> </ul>
Standard PEN		<ul style="list-style-type: none"> <li>•High <math>T_g</math></li> <li>•Few oriented chains</li> <li>•Low crystallinity</li> </ul>
Tensitized PEN		<ul style="list-style-type: none"> <li>•High <math>T_g</math></li> <li>•Many oriented chains</li> <li>•Low crystallinity</li> </ul>
ARAMID		<ul style="list-style-type: none"> <li>•Extremely high <math>T_g</math></li> <li>•Highly-rigid structure</li> <li>•Highly oriented chains</li> </ul>

$T_g$  for PET, PEN and ARAMID are 80, 120 and 280 °C, respectively according to DSC test.

The crystallinities for PET and PEN are 40-50 and 30-40 %, respectively.

**Figure 21** Schematic of molecular chain structures for various polymeric films.<sup>6</sup>

Japan, for helpful technical discussion during the research. Much of the work in this article was presented at the Information Storage Industry Consortium (INSIC) Tape Technology Road Map Meeting at Boulder, Colorado, September 2001.

## References

- Bhushan, B. *Mechanics and Reliability of Flexible Magnetic Media*, 2<sup>nd</sup> ed.; Springer-Verlag: New York, 2000.
- <http://www/lto-technology.com/newsite/html.format.html>.
- Richards, D. B.; Sharrock, M. P. *IEEE Trans Magn* 1998, 34, 1878–1882.
- Bhushan, B. *Tribology and Mechanics of Magnetic Storage Devices*, 2<sup>nd</sup> ed.; Springer-Verlag: New York, 1996.
- Bobji, M.; Bhushan, B. *J Mater Res* 2001, 16, 844–855.
- Higashioji, T.; Bhushan, B. *J Appl Polym Sci* 2002, 84, 1477–1498.
- Bhushan, B.; Ma, T.; Higashioji, T. *J Appl Polym Sci* 2002, 83, 2225–2244.
- Ma, T.; Bhushan, B.; Murooka, H.; Kobayashi, I.; Osawa, T. *Rev Sci Inst* 2002, 73, 1813–1820.
- Weick, B. L.; Bhushan, B. *J Appl Polym Sci* 2001, 81, 1142–1160.
- Weick, B. L.; Bhushan, B. *J Info Stor Proc Syst* 2000, 2, 207–220.
- Ma, T.; Bhushan, B. *J Appl Polym Sci*, in press.
- Ma, T.; Bhushan, B. *J Appl Polym Sci*, in press.
- Chen, D.; Zachmann, H. G. *Polymer* 1991, 32, 1612–1621.
- Ward, I. M.; Hadley, D. W. *An Introduction to the Mechanical Properties of Solid Polymers*; Wiley: New York, 1993.
- Storer, R. A. In *Annual Book of ASTM Standards*; American Society for Testing of Materials: West Conshohocken, PA, 1997; 14.02:348–351; 1999; 8.02:85–88.
- Osawa, T. Presented at the 8<sup>th</sup> NLIM Annual Review, Ohio State University, Oct. 30, 2001.
- Ezquerro, T. A.; Balta-Calleja, F. J.; Zachmann, H. G. *Acta Polym* 1993, 44, 18–24.
- Kunugi, T.; Watanabe, H.; Hashimoto, M. *J Appl Polym Sci* 1979, 24, 1039–1051.
- Gillmor J. R., Greener, J. *ANTEC* 1997, 45, 1582–1585.
- Williams, M. L.; Landel, R. F.; Ferry, J. D. *J Am Chem Soc* 1995, 77, 3701–3707.
- Ferry, J. D. *Viscoelastic Properties of Polymers*, 3<sup>rd</sup> ed.; Wiley: New York, 1980.
- Aklonis, J. J.; MacKnight, W. J. *Introduction to Polymer Viscoelasticity*; Wiley: New York, 1983.
- Higashioji, T.; Bhushan, B. *IEEE Trans Mag* 2001, 37, 1612–1615.
- Weick, B.; Bhushan, B. *J Appl Polym Sci* 1995, 58, 2381–2398.
- Murthy, N. S.; Bednarczyk, C.; Rim, P. B.; Nelson, J. *J Appl Polym Sci* 1997, 64, 1363–1371.
- Bhatt, G. M.; Bell, J. P. *J Polym Sci Polym Phys* 1976, 14, 575–590.
- Willson, M. P. *Polymer* 1974, 15, 277–282.
- Samuels, R. J. *J Polym Sci A-2* 1972, 10, 781–810.
- Cakmak, M.; Wang, Y. D. *J Appl Polym Sci* 1990, 41, 1867–1890.
- Mascia, L.; Fekkai, Z. *Polymer* 1993, 34, 1418–1422.